repeated treatment, thereby limiting the dose and treatment times of DTX-based therapy. In this study, DTX (10 mg/kg) was injected into rats via the tail vein [41], which is an amount the equivalent of five times greater than what is administered to humans. This led to 20% weight loss after 1 week, which required the discontinuation of the second administration of DTX. With regard to the findings from the DTX group in this study, the data from the tumor volume curves are controversial because the tumor volume in the DTX group was almost the same as in the control group (Fig. 2A). This was despite the results of our Western blot analysis for caspase 3 (Fig. 3C), which revealed that DTX was actually effective in inducing apoptosis in the tumor. Moreover, the tumor necrotic area in the DTX group tended to increase compared with that in the control group (Fig. 3B). Thus, although significant reduction of tumor volume was not observed, we consider that the administration of DTX was actually effective for inducing tumor necrosis and apoptosis.

Unlike DTX treatment, MCL thermotherapy heats tumor tissue without damaging neighboring normal tissues, and can therefore be performed safely and repeatedly. However, MCL thermotherapy has several problems that must be resolved before its application in the clinical setting, such as the development of AMF irradiation equipment appropriate for the human body, and an investigation into the safe use of MCLs. The injection of MCLs into tumor tissue becomes easier with the aid of three-dimensional CT or transrectal supersonic wave technology; however, for patients whose overall status is worsening, such as in cases of castration-resistant prostate cancer, administration by intravenous injection would be preferable. Unfortunately, owing to the large size of available MCLs (120–150 nm), intravenous injection is currently impossible. We are therefore attempting to minimize the size of MCLs. Finally, the development of a system capable of effectively guiding MCLs to the tumor region is necessary, and the effects of MCL thermotherapy must be examined using the spontaneous SOI model of metastasis that allows visualization of fluorescent protein prior to clinical application. If these problems can be resolved in the near future, the clinical application of MCL thermotherapy will be possible.

CONCLUSIONS

In summary, MCL thermotherapy heats only tumor tissue injected with MCLs, and is capable of inducing both necrotic and apoptotic cancer cell death, as well as tumor immunity, and suppressing bone destruction. In this study, the MCL thermotherapy group showed inhibition of bone destruction due to osteoclast induction compared with the control and DTX groups. Moreover, MCL thermotherapy inhibited cancer cell proliferation compared with that observed in the control and DTX groups, demonstrating that MCL thermotherapy can treat tumor cells and osteoclasts at the same time, as well as inhibit the vicious cycle of bone metastases. Finally, we showed that the combination of MCL thermotherapy and DTX treatment is much more effective than DTX monotherapy, suggesting that MCL thermotherapy should be adopted as a novel treatment for patients with bone metastatic prostate cancer in the future.

ACKNOWLEDGMENTS

This study was supported by a grant-in-Aid for Scientific Research (C) No. 21592055 and No. 21790390 from the Ministry of Education, Culture, Sports, Science and Technology of Japan, a grant-in-aid for Research at Nagoya City University, a grant-in-aid from Ichihara International Scholarship Foundation, and a grant-in-aid from Aichi Cancer Research Foundation. We thank Noritaka Yoshikawa (Olympus Medical Science Sale Co., Ltd.) who provided CT for animal experiments of bone evaluation and thermography for temperature evaluations. We also thank Koji Kato, Engineer (Department of Experimental Pathology, Nagoya City University Graduate School of Medical Sciences) and Ayano Yoshida (College of Bioscience and Biotechnology, Chubu University) for technical assistance.

REFERENCES

1. Bubendorf L, Schopfer A, Wagner U, Sauter G, Moch H, Willi N, Gasser TC, Mihatsch MJ. Metastatic patterns of prostate cancer: An autopsy study of 1,589 patients. Hum Pathol 2000; 31:578–583.
2. Mehra R, Kumar-Sinha C, Shankar S, Lonigro RJ, Jing X, Philips NE, Siddiqui J, Han B, Cao X, Smith DC, Shah RB, Chinnaiyan AM, Pienta KJ. Characterization of bone metastases from rapid autopsies of prostate cancer patients. Clin Cancer Res 2011;17:3924–3932.
3. Saad F, Clarke N, Colombel M. Natural history and treatment of bone complications in prostate cancer. Eur Urol 2006;49: 429–440.
4. Jemal A, Siegel R, Xu J, Ward E. Cancer statistics, 2010. CA Cancer J Clin 2010;60:277–300.
5. Kingsley LA, Fournier PG, Chirgwin JM, Guise TA. Molecular biology of bone metastasis. Mol Cancer Ther 2007;6:2609–2617.
6. Kozlow W, Guise TA. Breast cancer metastasis to bone: Mechanisms of osteolysis and implications for therapy. J Mammary Gland Biol Neoplasia 2005;10:169–180.
7. Yoneda T, Hiraga T. Crosstalk between cancer cells and bone microenvironment in bone metastasis. Biochem Biophys Res Commun 2005;328:679–687.
8. Finkelman RD, Mohan S, Jennings JC, Taylor AK, Jepsen S, Baylink DJ. Quantitation of growth factors IGF-I, SGF/IGF-II,

and TGF-beta in human dentin. J Bone Miner Res 1990;5: 717–723.

9. Sato S, Futakuchi M, Ogawa K, Asamoto M, Nakao K, Asai K, Shirai T. Transforming growth factor beta derived from bone matrix promotes cell proliferation of prostate cancer and osteoclast activation-associated osteolysis in the bone microenvironment. Cancer Sci 2008;99:316–323.
10. Solheim E. Growth factors in bone. Int Orthop 1998;22:410–416.
11. Berry S, Waldron T, Winquist E, Lukka H. The use of bisphosphonates in men with hormone-refractory prostate cancer: A systematic review of randomized trials. Can J Urol 2006;13:3180–3188.
12. Saad F, McKiernan J, Eastham J. Rationale for zoledronic acid therapy in men with hormone-sensitive prostate cancer with or without bone metastasis. Urol Oncol 2006;24:4–12.
13. Fizazi K, Carducci M, Smith M, Damiao R, Brown J, Karsh L, Milecki P, Shore N, Rader M, Wang H, Jiang Q, Tadros S, Dansey R, Goessl C. Denosumab versus zoledronic acid for treatment of bone metastases in men with castration-resistant prostate cancer: A randomised, double-blind study. Lancet 2011;377:813–822.
14. Kusaka M, Takegami K, Sudo A, Yamazaki T, Kawamura J, Uchida A. Effect of hyperthermia by magnetite cement on tumor-induced bone destruction. J Orthop Sci 2002;7:354–357.
15. Abe M, Hiraoka M, Takahashi M, Egawa S, Matsuda C, Onoyama Y, Morita K, Kakehi M, Sugahara T. Multi-institutional studies on hyperthermia using an 8-MHz radiofrequency capacitive heating device (Thermotron RF-8) in combination with radiation for cancer therapy. Cancer 1986; 58:1589–1595.
16. Kawai N, Futakuchi M, Yoshida T, Ito A, Sato S, Naiki T, Honda H, Shirai T, Kohri K. Effect of heat therapy using magnetic nanoparticles conjugated with cationic liposomes on prostate tumor in bone. Prostate 2008;68:784–792.
17. Kawai N, Ito A, Nakahara Y, Futakuchi M, Shirai T, Honda H, Kobayashi T, Kohri K. Anticancer effect of hyperthermia on prostate cancer mediated by magnetite cationic liposomes and immune-response induction in transplanted syngeneic rats. Prostate 2005;64:373–381.
18. Kawai N, Ito A, Nakahara Y, Honda H, Kobayashi T, Futakuchi M, Shirai T, Tozawa K, Kohri K. Complete regression of experimental prostate cancer in nude mice by repeated hyperthermia using magnetite cationic liposomes and a newly developed solenoid containing a ferrite core. Prostate 2006;66:718–727.
19. Yanase M, Shinkai M, Honda H, Wakabayashi T, Yoshida J, Kobayashi T. Intracellular hyperthermia for cancer using magnetite cationic liposomes: An in vivo study. Jpn J Cancer Res 1998;89:463–469.
20. Shirai T, Tamano S, Kato T, Iwasaki S, Takahashi S, Ito N. Induction of invasive carcinomas in the accessory sex organs other than the ventral prostate of rats given 3,2'-dimethyl-4-aminobiphenyl and testosterone propionate. Cancer Res 1991; 51:1264–1269.
21. Sato S, Takahashi S, Asamoto M, Naiki T, Naiki-Ito A, Asai K, Shirai T. Tranilast suppresses prostate cancer growth and osteoclast differentiation in vivo and in vitro. Prostate 2010;70:229–238.
22. Owen CS, Sykes NL. Magnetic labeling and cell sorting. J Immunol Methods 1984;73:41–48.
23. Shinkai M, Yanase M, Honda H, Wakabayashi T, Yoshida J, Kobayashi T. Intracellular hyperthermia for cancer using magnetite cationic liposomes: In vitro study. Jpn J Cancer Res 1996;87:1179–1183.
24. Sorensen AG, Patel S, Harmath C, Bridges S, Synnott J, Sievers A, Yoon YH, Lee EJ, Yang MC, Lewis RF, Harris GJ, Lev M, Schaefer PW, Buchbinder BR, Barest G, Yamada K, Ponzo J, Kwon HY, Gemmete J, Farkas J, Tievsky AL, Ziegler RB, Salhus MR, Weisskoff R. Comparison of diameter and perimeter methods for tumor volume calculation. J Clin Oncol 2001;19:551–557.
25. Jensen MM, Jorgensen JT, Binderup T, Kjaer A. Tumor volume in subcutaneous mouse xenografts measured by microCT is more accurate and reproducible than determined by 18F-FDG-microPET or external caliper. BMC Med Imaging 2008;8:16.
26. Mundy GR. Metastasis to bone: Causes, consequences and therapeutic opportunities. Nat Rev Cancer 2002;2:584–593.
27. Fu X, Herrea H, Hoffman RM. Orthotopic growth and metastasis of human prostate carcinoma in nude mice after transplantation of histologically intact tissue. Int J Cancer 1992;52:987–990.
28. Hoffman RM. Orthotopic metastatic mouse models for anticancer drug discovery and evaluation: A bridge to the clinic. Invest New Drugs 1999;17:343–359.
29. Yang M, Jiang P, Yamamoto N, Li L, Geller J, Moossa AR, Hoffman RM. Real-time whole-body imaging of an orthotopic metastatic prostate cancer model expressing red fluorescent protein. Prostate 2005;62:374–379.
30. Hoffman RM. The multiple uses of fluorescent proteins to visualize cancer in vivo. Nat Rev Cancer 2005;5:796–806.
31. Hoffman RM, Yang M. Whole-body imaging with fluorescent proteins. Nat Protoc 2006;1:1429–1438.
32. Mukhopadhaya A, Mendecki J, Dong X, Liu L, Kalnicki S, Garg M, Alfieri A, Guha C. Localized hyperthermia combined with intratumoral dendritic cells induces systemic antitumor immunity. Cancer Res 2007;67:7798–7806.
33. Ito A, Shinkai M, Honda H, Yoshikawa K, Saga S, Wakabayashi T, Yoshida J, Kobayashi T. Heat shock protein 70 expression induces antitumor immunity during intracellular hyperthermia using magnetite nanoparticles. Cancer Immunol Immunother 2003;52:80–88.
34. Radons J, Multhoff G. Immunostimulatory functions of membrane-bound and exported heat shock protein 70. Exerc Immunol Rev 2005;11:17–33.
35. Udono H, Levey DL, Srivastava PK. Cellular requirements for tumor-specific immunity elicited by heat shock proteins: Tumor rejection antigen gp96 primes CD8+ T cells in vivo. Proc Natl Acad Sci USA 1994;91:3077–3081.
36. Suto R, Srivastava PK. A mechanism for the specific immunogenicity of heat shock protein-chaperoned peptides. Science 1995;269:1585–1588.
37. Subjeck JR, Sciandra JJ, Chao CF, Johnson RJ. Heat shock proteins and biological response to hyperthermia. Br J Cancer Suppl 1982;5:127–131.
38. Subjeck JR, Sciandra JJ, Johnson RJ. Heat shock proteins and thermotolerance; A comparison of induction kinetics. Br J Radiol 1982;55:579–584.
39. Lindquist S. The heat-shock response. Annu Rev Biochem 1986;55:1151–1191.
40. Horowitz M, Robinson SD. Heat shock proteins and the heat shock response during hyperthermia and its modulation by altered physiological conditions. Prog Brain Res 2007;162: 433–446.
41. Wonganan P, Zamboni WC, Strychor S, Dekker JD, Croyle MA. Drug–virus interaction: Effect of administration of recombinant adenoviruses on the pharmacokinetics of docetaxel in a rat model. Cancer Gene Ther 2009;16:405–414.

IJC
International Journal of Cancer

2-Amino-1-methyl-6-phenylimidazo[4,5-b]pyridine (PhIP)-DNA adducts in benign prostate and subsequent risk for prostate cancer

Deliang Tang[1], Oleksandr N. Kryvenko[2], Yun Wang[3], Sheri Trudeau[3], Andrew Rundle[4], Satoru Takahashi[5], Tomoyuki Shirai[5] and Benjamin A. Rybicki[3]

[1] Department of Environmental Health Sciences, Columbia University, New York, NY
[2] Department of Pathology, Henry Ford Health System, Detroit, MI
[3] Department of Public Health Sciences, Henry Ford Health System,, Detroit, MI
[4] Department of Epidemiology, Columbia University, New York, NY
[5] Department of Pathology, Nagoya City University Medical School, Nagoya, Japan

Despite convincing evidence that 2-amino-1-methyl-6-phenylimidazo[4,5-b]pyridine (PhIP)—a heterocyclic amine generated by cooking meats at high temperatures—is carcinogenic in animal models, it remains unclear whether PhIP exposure leads to increased cancer risk in humans. PhIP-DNA adduct levels were measured in specimens from 534 prostate cancer case-control pairs nested within a historical cohort of men with histopathologically benign prostate specimens. We estimated the overall and race-stratified risk of subsequent prostate cancer associated with higher adduct levels. PhIP-DNA adduct levels in benign prostate were significantly higher in Whites than African Americans (0.274 optical density units (OD) ±0.059 *vs.* 0.256 OD ±0.054; $p<0.0001$). Prostate cancer risk for men in the highest quartile of PhIP-DNA adduct levels was modestly increased [odds ratio (OR) = 1.25; 95% confidence interval (CI) = 0.76–2.07]. In subset analyses, the highest risk estimates were observed in White patients diagnosed more than 4 years after cohort entry (OR = 2.74; 95% CI = 1.01–7.42) or under age 65 (OR = 2.80; 95% CI = 0.87–8.97). In Whites, cancer risk associated with high-grade prostatic intraepithelial neoplasia combined with elevated PhIP-DNA adduct levels (OR = 3.89; 95% CI = 1.56–9.73) was greater than risk associated with either factor alone. Overall, elevated levels of PhIP-DNA adducts do not significantly increase prostate cancer risk. However, our data show that White men have higher PhIP-DNA adduct levels in benign prostate tissue than African American men, and suggest that in certain subgroups of White men high PhIP-DNA adduct levels may predispose to an increased risk for prostate cancer.

2-Amino-1-methyl-6-phenylimidazo[4,5-*b*]pyridine (PhIP) is the most abundant heterocyclic amine (HCA) formed during the cooking of meat,[1] and a potential dietary risk factor for prostate and other cancers. A direct correlation between PhIP exposure, DNA adduct formation and other indicators of prostate carcinogenesis is supported by animal models and *in vitro* studies of human tissues. Rats fed a PhIP-laden diet for 52 weeks had PhIP-DNA adducts in all prostate lobes and subsequently developed prostate cancer[2]; PhIP exposure in rats is also associated with elevated mutation frequencies in prostate tissue[3] and increased prostate tumor incidence.[4] Mice administered PhIP showed positive staining for PhIP-DNA adducts in human prostate xenografts.[5] More recently, inflammation, atrophy of acini and prostatic intraepithelial neoplasia were observed in the prostate glands of a *CYP1A*-humanized mouse model, following a single oral dose of PhIP.[6]

Several *in vitro* studies of human prostate tissue incubated in PhIP-laden milieu have demonstrated detectable PhIP-DNA adducts in prostate cells.[7–9] While one study found a low prevalence of detectable PhIP-DNA adducts in prostate tissue using the ^{32}P-postlabeling method,[10] our own studies have demonstrated that PhIP-DNA adduct levels in prostate are related to dietary intake[11,12] and tumor grade.[13] *In vitro* experiments using the comet assay, and human prostate epithelial cells have shown that increased doses of PhIP result in increased DNA damage.[14] A study using a modified *in vitro* mutagen sensitivity assay, with activated PhIP (N-OH-PhIP) as the challenge mutagen and chromosomal aberrations as

Key words: dNA adducts, nested case–control study, immunohistochemistry, carcinogens, imidazoles, biopsy, needle

Abbreviations: BSA: bovine serum albumin; CI: confidence interval; HCA: heterocyclic amine; HGPIN: high-grade prostatic intraepithelial neoplasia; OD: optical density units; OR: odds ratio; PhIP: 2-amino-1-methyl-6-phenylimidazo[4,5-b]pyridine; PSA: prostate specific antigen; UGT: UDP-glucuronosyltransferases

Additional supporting information may be found in the online version of this article.

Grant sponsor: National Institutes of Health; **Grant number:** 5R01-ES011126

DOI: 10.1002/ijc.28092

History: Received 23 Nov 2012; Accepted 16 Jan 2013; Online 7 Feb 2013

Correspondence to: Benjamin A. Rybicki, PhD, One Ford Place 3E, Detroit, Michigan 48202, USA, Tel.: 313–874-6360, Fax: +313–874-6730, E-mail: brybick1@hfhs.org

What's new?

While exposure to high levels of PhIP (2-amino-1-methyl-6-phenylimidazo[4,5-b]pyridine)—a heterocyclic amine found in cooked meat—is associated with the development of prostate malignancies in animals, it is unclear whether this same risk exists in humans. Here, risk of prostate cancer in men was found to be increased only in the presence of both glandular inflammation and elevated levels of PhIP-DNA adducts, based on analysis of benign prostate specimens. However, certain subgroups of White males, who had higher PhIP-DNA adduct levels than African Americans, may be at greater risk for the disease. Given the putative role of inflammation in cancer, targeted prevention strategies in men with known high PhIP exposure levels may lead to beneficial health outcomes.

the endpoint, found that prostate cancer cases showed significantly higher numbers of breaks,[15] suggesting a greater susceptibility to PhIP-induced carcinogenesis in prostate cancer cases.

Despite the strong evidence for PhIP-induced prostate carcinogenesis from animal and *in vitro* studies, studies of dietary PhIP exposure and human prostate cancer risk are largely equivocal.[16–21] One limitation of these studies is their reliance on food frequency questionnaires to estimate PhIP exposure. While dietary intake data is informative, it is ultimately a poor measure of biologically effective dose, as it does not account for individual variation in PhIP metabolism or DNA repair capacity, which can influence DNA adduct formation.[11] Cellular and molecular changes are likely to be more relevant to disease outcome than measurement of PhIP in the diet. As such, the detection and quantification of PhIP-DNA adducts within the tissue of interest is an important step toward understanding the connection between exposure and cancer development. Case-control studies of PhIP-DNA adducts and cancer risk are limited to two studies, one of breast[22] and the other of pancreas,[23] both of which found elevated PhIP-DNA adducts in cancer patients. No studies have examined PhIP-DNA adducts levels in benign tissue and subsequent prostate cancer risk. Our own previous research on PhIP-DNA adduct levels was a cross-sectional study without a control group, using prostate tissue from cancer cases.[11–13]

In this study, we advance the molecular epidemiologic study of DNA adducts and cancer risk by measuring PhIP-DNA adduct levels in histopathologically normal tissue specimens taken from the target organ, and assess the relationship between adduct levels, pre-neoplastic histological markers, and subsequent cancer risk using a case-control study nested within a large historical cohort. In addition to testing whether adduct levels in histopathologically benign target tissue were associated with incident prostate cancer and tumor aggressiveness, we also explored race-specific cancer associations.

Epidemiology

Methods

Study sample and medical record review

After obtaining approval from the Henry Ford Health System Institutional Review Board, we identified a historical cohort of 6,692 men with a benign prostate specimen collected by needle core biopsy or transurethral resection of the prostate (TURP) between January 1990 and December 2002. A nested case–control sample was drawn from this cohort based on eligibility criteria that included a recorded prostate specific antigen (PSA) level within a year of cohort entry and no history of a previous prostate cancer diagnosis. "Date of cohort entry" was defined as the date that the initial benign prostate specimen was acquired; "date of case diagnosis" was the date of first cancer-positive tissue specimen or the date a clinician first reported a clinical diagnosis of prostate cancer. Patients diagnosed with prostate cancer less than one year from date of cohort entry were ineligible for the study. We identified 808 potentially eligible cases diagnosed with prostate cancer prior to July 2007.

Incidence density sampling was used to select controls without replacement from all cohort members at risk at the time of case occurrence. Controls were randomly selected from among those cohort members who were free of prostate cancer at a follow-up duration greater than or equal to the time between cohort entry and diagnosis dates of the matched cases, with the end of follow-up denoted as the "reference date" for controls. Matching criteria included age at entry into cohort (±2 years), date of entry into cohort (±2 years), race (African American or White) and type of specimen (biopsy or TURP). We were able to match 802 of 808 potentially eligible cases. Further review reduced the final analytic sample to 574 case-control pairs,[24] of which we were able to analyze the PhIP-DNA adduct levels in 534 pairs; the remaining 40 pairs were excluded due to absence of sufficient numbers of epithelial cells in the tissue specimen.

Smoking status, and clinical, demographic, and co-morbidity data were abstracted from patients' medical records from 5 years before the date of cohort entry through the date of diagnosis (for prostate cancer cases) or reference date (for controls). All medical data used in study analyses are based on the date of cohort entry unless otherwise noted.

Immunohistochemistry

Consecutive sections (5-micron thick) were cut from each formalin-fixed, paraffin-embedded prostate specimen; one slide was used for PhIP-DNA adduct detection as described below and the other was hematoxylin and eosin (H&E) stained and examined by a single genitourinary pathologist

(O.N.K.) blinded to disease progression. The pathology examination included evaluation of the specimen for the presence of cancer, high-grade prostatic intraepithelial neoplasia (HGPIN), atrophy, and inflammation.[24]

Paraffin-embedded sections were heated to 50°C for 1 hr, deparaffinized in xylene, and rehydrated in serial alcohol. After treatment with RNase and Proteinase K, the sections were blocked using 3% bovine serum albumin (BSA) and normal goat serum. Sections were incubated in a humid 4°C chamber overnight with a 1:500 dilution of the primary anti-PhIP-DNA adduct polyclonal antibody[2,25]; then incubated at room temperature for 30 min with a 1:200 dilution of the biotinylated secondary antibody. Specimens were bathed in 0.3% hydrogen peroxide in methanol for 20 min to block endogenous peroxidase activity.

The PhIP-DNA polyclonal antibody recognizes DNA adducts at the C8 position of deoxyguanosine as the epitope. The PhIP-modified DNA antigen contains N^2-(2′-deoxyguanosin-8-yl)-PhIP,[25] which is recognized as the major adduct formed between PhIP and DNA.[26] Specificity of the PhIP-DNA adduct antibody was evaluated in liver tissue of rats separately exposed for 6 weeks to HCAs as follows: 3-amino-1,4-dimethyl-5H-pyrido[4,3-b]indole (Trp-P-1, 150ppm); 2-aminodipyrido[1,2-a:3',2'-d]imidazole (Glu-P-2, 500ppm); 2-amino-3-methylimidazo[4,5-f]quinoline (MeIQ, 300ppm); or 2-amino-3,8-dimethylimidazo[4,5-f]quinoxaline (MeIQx, 400ppm). Presence of DNA adducts was confirmed by the ^{32}P-postlabeling method.[27] No cross-reactivity with any HCA-DNA adducts was found (S. Takahashi, unpublished data).

The antibody complex was detected using an avidin-biotin-peroxidase complex solution and visualized using 3,3'-diaminobenzidine chromogen (Zymed Laboratories, San Francisco, CA). A negative control was included in each experiment by omitting the primary antibody. A cytospin sample of MCF-7 cells without PhIP treatment was included in each batch of staining. Staining was measured by absorbance image analysis using the Cell Analysis System 200 (Becton Dickinson, San Jose, CA). Absorbance of light at a wavelength of 500 nmol/L was measured in optical density units (OD). Previous calibration studies using N-hydroxy-PhIP-treated MCF-7 cells have demonstrated optical density sensitivity to N-hydroxy-PhIP adducts ranging from 1 to 100 μM with a detection limit of about $1/10^7$ for PhIP-DNA adducts.[22] For each specimen, a technician scored 50 epithelial cells (five fields, ten cells per field) selected to be representative, in terms of intensity, of the cells in the field.

Statistical analysis

Conditional logistic regression analyses were used to estimate both unadjusted and adjusted odds ratios (ORs) for prostate cancer incidence during follow-up. Individual matching controlled for age, race, and specimen type (biopsy or TURP). Analyses were performed using adduct levels expressed as both continuous and categorical variables; for the latter, adduct distribution was segmented among control subjects into referent categories. Potential confounders were identified by first testing whether the variable was associated with case status or adduct levels; associated variables were then tested in multivariable models to determine whether their inclusion changed the effect estimate by 10% or more. Comparisons between stratified models were assessed using conditional logistic regression with interaction terms.

Results

Study sample and PhIP-DNA adduct levels

In the analytic sample of 534 pairs, cases were an average of 65.4 years old at cohort entry and 40% were African American (supporting information Table 1). The 40 pairs with unanalyzable adduct data were significantly older (2.5 years, $p = 0.05$), had 0.8 more PSA tests between cohort entry and diagnosis ($p = 0.05$), and entered the cohort earlier (median 21 months, $p = 0.03$) than those that were analyzed. In the full sample, median time to diagnosis was 1–4 years after cohort entry, with the remaining cases diagnosed 4–15 years after cohort entry. Cases had significantly higher PSA levels at time of cohort entry (7.7 ± 7.3 ng/mL *vs.* 5.6 ± 5.3 ng/mL; $p < 0.0001$) and averaged two more PSA tests between cohort entry and diagnosis. The majority of cases (52.6%) had Stage 2 tumors; 29% of cases had advanced tumor grade defined as either Gleason score 8 and above or Gleason score 7 with a primary Grade 4. Mean PhIP-DNA adduct levels were slightly elevated in cases compared with controls, but the difference was not statistically significant (0.263 OD ± 0.058 *vs.* 0.260 OD ± 0.045; $p = 0.32$).

Factors associated with PhIP-DNA adduct levels

Given the known association between race and differences in both exposure to and metabolism of PhIP,[13,28–30] we tested whether PhIP-DNA adduct levels varied by race. Mean adduct levels were significantly higher in Whites than African Americans (0.276 ± 0.059 *vs.* 0.257 ± 0.053 OD; $p < 0.0001$) and followed a normal distribution in both racial groups (supporting information Figure 1).

To better understand how the histological characteristics of prostate tissue might affect PhIP-DNA adduct levels, we estimated the mean adduct levels by histological variables that were previously described in this sample (Table 1).[24] In White patients with partial atrophy, we observed significantly higher levels of PhIP-DNA adducts than in those without partial atrophy (0.285 ± 0.060 *vs.* 0.272 ± 0.059 OD; $p = 0.01$); the same trend in adduct levels was observed in the benign prostate specimens derived from African American patients, but differences between groups were smaller. Conversely, in African Americans with glandular inflammation, adduct levels were significantly higher than in those without glandular inflammation (0.239 ± 0.057 *vs.* 0.260 ± 0.051 OD; $p = 0.005$), and a similar, but less significant inverse association was observed in Whites. In an effort to further tease apart the association of atrophy with adduct

Table 1. Mean PhIP-DNA adduct levels in optical density units stratified by race and histological variables

	Mean optical density units ± standard deviation								
	Whole sample			African Americans			Whites		
Variable	Present	Absent	*p* value	Present	Absent	*p* value	Present	Absent	*p* value
HGPIN	0.272 ± .054 ($n = 74$)	0.268 ± .058 ($n = 838$)	0.60	0.253 ± .048 ($n = 31$)	0.257 ± .053 ($n = 323$)	0.69	0.285 ± .055 ($n = 43$)	0.275 ± .060 ($n = 515$)	0.28
Atrophy	0.269 ± .058 ($n = 736$)	0.266 ± .058 ($n = 176$)	0.45	0.257 ± .054 ($n = 285$)	0.256 ± .049 ($n = 69$)	0.86	0.277 ± .059 ($n = 451$)	0.272 ± .063 ($n = 107$)	0.43
Simple atrophy	0.269 ± .057 ($n = 656$)	0.269 ± .060 ($n = 256$)	0.95	0.256 ± .053 ($n = 253$)	0.260 ± .051 ($n = 101$)	0.51	0.277 ± .057 ($n = 403$)	0.274 ± .065 ($n = 155$)	0.62
Post-atrophic hyperplasia	0.282 ± .050 ($n = 18$)	0.268 ± .058 ($n = 894$)	0.34	0.308 ± .021 ($n = 3$)	0.257 ± .053 ($n = 351$)	0.09	0.276 ± .053 ($n = 15$)	0.279 ± .060 ($n = 543$)	0.99
Simple atrophy—cyst formation	0.264 ± .061 ($n = 175$)	0.270 ± .057 ($n = 737$)	0.28	0.258 ± .064 ($n = 54$)	0.257 ± .050 ($n = 300$)	0.88	0.267 ± .060 ($n = 121$)	0.279 ± .059 ($n = 437$)	0.07
Partial atrophy	0.277 ± .059 ($n = 267$)	0.265 ± .057 ($n = 645$)	0.006	0.260 ± .051 ($n = 91$)	0.256 ± .053 ($n = 263$)	0.45	0.285 ± .060 ($n = 176$)	0.272 ± .059 ($n = 382$)	0.01
Inflammation	0.267 ± .056 ($n = 551$)	0.272 ± .059 ($n = 361$)	0.18	0.254 ± .053 ($n = 219$)	0.261 ± .051 ($n = 135$)	0.24	0.275 ± .057 ($n = 332$)	0.278 ± .063 ($n = 226$)	0.48
Glandular inflammation	0.259 ± .059 ($n = 169$)	0.271 ± .057 ($n = 743$)	0.02	0.239 ± .057 ($n = 56$)	0.260 ± .051 ($n = 298$)	0.005	0.270 ± .058 ($n = 113$)	0.278 ± .060 ($n = 445$)	0.18
Periglandular inflammation	0.264 ± .058 ($n = 364$)	0.272 ± .057 ($n = 548$)	0.04	0.251 ± .055 ($n = 148$)	0.262 ± .051 ($n = 206$)	0.05	0.273 ± .058 ($n = 216$)	0.278 ± .060 ($n = 342$)	0.31
Stromal inflammation	0.266 ± .056 ($n = 430$)	0.271 ± .059 ($n = 482$)	0.19	0.254 ± .053 ($n = 171$)	0.259 ± .052 ($n = 183$)	0.39	0.274 ± .056 ($n = 259$)	0.278 ± .063 ($n = 299$)	0.37

Table 2. Association of PhIP-DNA Adduct Levels with Prostate Cancer

Sample	OR[1]	95% CI	*p* value
PhIP-DNA adduct Level			
Whole sample ($n = 534$ case–control pairs)			
2nd Quartile	1.20	0.83–1.72	0.34
3rd Quartile	1.29	0.87–1.92	0.20
4th Quartile	1.25	0.76–2.07	0.38
Trend test			0.36
High PhIP level[2]	1.16	0.84–1.59	0.37
African Americans ($n = 213$ case–control pairs)			
2nd Quartile	1.32	0.75–2.32	0.33
3rd Quartile	0.96	0.49–1.86	0.90
4th Quartile	0.73	0.32–1.63	0.44
Trend test			0.35
High PhIP level[1]	0.76	0.44–1.32	0.33
Whites ($n = 321$ case–control pairs)			
2nd Quartile	1.12	0.69–1.81	0.65
3rd Quartile	1.48	0.90–2.44	0.13
4th Quartile	1.73	0.89–2.34	0.10
Trend Test			0.07
High PhIP level[2]	1.44	0.97–2.14	0.07

[1]All risk estimates use lowest level as referent group.
[2]Above median level in controls.

levels, we modeled PhIP-DNA adduct levels with covariates for both simple and partial atrophy adjusting for race and glandular inflammation. The least squares mean estimates of PAH-DNA adduct levels for the four possible combinations of simple and partial atrophy are shown in Figure 1. In cases, PhIP-DNA adduct levels were lowest when no atrophy was present, highest when only partial atrophy was present, and intermediate when simple atrophy was present (irrespective of whether partial atrophy was also present). In controls, there was no association between PhIP-DNA adduct levels and atrophy status; controls had higher levels of PhIP-DNA adducts than cases when no atrophy was observed, but much lower levels than cases when only partial atrophy was noted in the specimen. This same general pattern was observed when the data were stratified by race.

Prostate cancer risk associated with higher levels of PhIP-DNA adducts

While mean PhIP-DNA adduct levels did not differ significantly between cases and controls, previous studies have shown that the effect of DNA adducts on cancer-related outcomes tends to be non-linear.[31,32] Therefore, to determine whether prostate cancer risk was associated with elevated adduct levels, we tested two models, one in which adduct levels were categorized into quartiles, and another in which levels were dichotomized above and below the median (Table 2). Due to the differences of adduct levels by race, models for both the full sample as well as race-stratified models were tested. For the full sample, quartile risk estimates did not reach statistical significance nor was the trend statistically significant ($p = 0.36$); similarly, the OR for adduct levels greater than the median was also non-significant. When the sample was stratified by race, increased risk associated with elevated PhIP-DNA adduct levels trended upward in Whites: 12% for the 2nd quartile, 48% for the 3rd quartile, and 73% for the 4th quartile, but none were statistically significant, nor was the trend statistically significant ($p = 0.07$). Models adjusting for inflammation, atrophy, and number of PSA tests were also tested, but changes in risk estimates were nominal (data not shown).

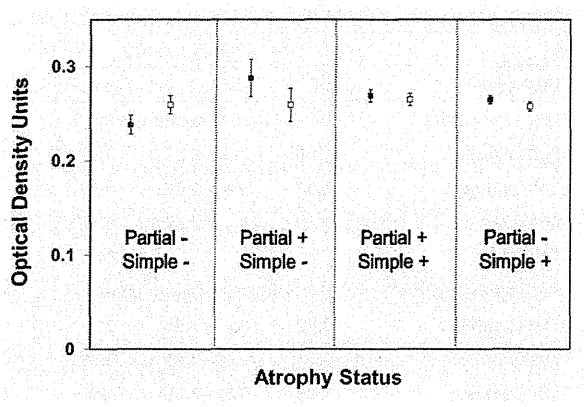

Figure 1. Least squares means estimates of PhIP-DNA adduct levels by case (shaded square)/control (open square) status and type of atrophy in the benign sample.

Table 3 reports risk estimates stratified by selected matching factors (including race) and tumor grade (for cases). In the full sample, little evidence for heterogeneity of high PhIP-DNA adduct levels by strata exists. In the White subsample—where elevated PhIP-DNA adduct levels had suggestive associations with prostate cancer risk—ORs were greater for cases with high tumor grade, longer follow-up, later cohort entry, and younger age at diagnosis. In White cases diagnosed before age 65, the risk of prostate cancer was elevated 70–80% in the 2nd and 3rd quartiles, and 180% in the 4th quartile, but neither risk estimates nor the linear trend test reached statistical significance.

The other stratum with markedly higher risk estimates was White cases diagnosed 4 years or more after cohort entry, where risk of prostate cancer was unchanged for the 2nd quartile, but increased 60% for the 3rd quartile and 174% for the 4th quartile. The risk estimate in the 4th quartile was marginally statistically significant [OR = 2.74; 95% confidence interval (CI) = 1.01–7.42] and the linear trend of risk estimates across quartiles was also statistically significant ($p = 0.03$). To further investigate whether this suggested a temporal relationship between adduct levels and prostate cancer, we analyzed the association between adduct quartile and

Table 3. Association of PhIP-DNA adduct levels with prostate cancer, stratified by matching factors and case characteristics

Sample	Whole sample			African Americans			Whites		
PhIP Level	OR[1]	95% CI	*p* value	OR	95% CI	*p* value	OR	95% CI	*p* value
Low tumor grade	(*n* = 367 case–control pairs)			(*n* = 137 case–control pairs)			(*n* = 230 case–control pairs)		
2nd Quartile	1.40	0.84–2.31	0.19	1.94	0.83–4.55	0.13	1.17	0.62–2.19	0.63
3rd Quartile	1.37	0.81–2.33	0.25	1.42	0.53–3.85	0.49	1.30	0.69–2.46	0.41
4th Quartile	1.29	0.65–2.54	0.47	1.09	0.30–4.01	0.90	1.36	0.61–3.04	0.46
Trend test			0.51			0.98			0.43
High tumor grade	(*n* = 138 case–control pairs)			(*n* = 56 case–control pairs)			(*n* = 82 case–control pairs)		
2nd Quartile	0.92	0.45–1.86	0.81	1.14	0.38–3.44	0.82	0.87	0.33–2.28	0.77
3rd Quartile	1.57	0.68–3.65	0.29	0.94	0.22–4.08	0.93	2.04	0.69–6.07	0.20
4th Quartile	1.03	0.31–3.39	0.97	0.45	0.07–2.96	0.41	1.84	0.34–10.00	0.48
Trend test		0.76			0.43			0.33	
1–4 years of Follow-up	(*n* = 266 case–control pairs)			(*n* = 103 case–control pairs)			(*n* = 163 case–control pairs)		
2nd Quartile	1.63	0.91–2.92	0.10	1.83	0.76–4.44	0.18	1.48	0.68–3.24	0.32
3rd Quartile	1.46	0.75–2.84	0.27	0.99	0.31–3.16	0.99	1.68	0.74–3.84	0.22
4th Quartile	1.15	0.49–2.69	0.74	0.95	0.23–4.02	0.95	1.23	0.42–3.55	0.71
Trend test			0.82			0.75			0.67
4–15 years of follow-up	(*n* = 267 case–control pairs)			(*n* = 110 case–control pairs)			(*n* = 157 case–control pairs)		
2nd Quartile	0.90	0.51–1.58	0.72	0.82	0.32–2.11	0.67	0.99	0.48–2.05	0.99
3rd Quartile	1.34	0.75–2.37	0.32	0.90	0.32–2.55	0.84	1.60	0.78–3.27	0.20
4th Quartile	1.46	0.70–3.03	0.31	0.62	0.17–2.18	0.45	2.74	1.01–7.42	0.05
Trend test			0.21			0.53			0.03
Early cohort entry	(*n* = 263 case–control pairs)			(*n* = 88 case–control pairs)			(*n* = 175 case–control pairs)		
2nd Quartile	1.28	0.69–2.40	0.44	2.46	0.69–8.76	0.17	1.02	0.49–2.12	0.96
3rd Quartile	1.28	0.68–2.40	0.44	1.92	0.56–6.53	0.30	1.09	0.52–2.29	0.83
4th Quartile	1.73	0.78–3.86	0.18	2.76	0.60–12.75	0.19	1.42	0.54–3.72	0.48
Trend test			0.21			0.27			0.47
Late cohort entry	(*n* = 270 case–control pairs)			(*n* = 125 case–control pairs)			(*n* = 145 case–control pairs)		
2nd Quartile	1.10	0.67–1.84	0.69	1.00	0.48–2.10	1.00	1.14	0.55–2.36	0.72
3rd Quartile	1.40	0.76–2.57	0.28	0.60	0.20–1.77	0.35	2.18	0.99–4.78	0.05
4th Quartile	0.98	0.46–2.13	0.97	0.29	0.08–1.08	0.06	2.14	0.73–6.24	0.16
Trend test			0.89			0.06			0.09
Age <65	(*n* = 274 case–control pairs)			(*n* = 110 case–control pairs)			(*n* = 164 case–control pairs)		
2nd Quartile	1.30	0.72–2.35	0.39	0.92	0.38–2.24	0.85	1.79	0.79–4.09	0.16
3rd Quartile	1.35	0.72–2.53	0.35	0.95	0.35–2.60	0.92	1.71	0.74–3.95	0.21
4th Quartile	1.08	0.47–2.47	0.85	0.38	0.10–1.42	0.15	2.80	0.87–8.97	0.08
Trend test			0.83			0.18			0.09
Age 65+	(*n* = 259 case–control pairs)			(*n* = 103 case–control pairs)			(*n* = 156 case–control pairs)		
2nd Quartile	1.10	0.64–1.89	0.72	1.71	0.65–4.50	0.27	0.82	0.41–1.62	0.56
3rd Quartile	1.45	0.79–2.67	0.23	1.02	0.29–3.60	0.97	1.55	0.76–3.16	0.22
4th Quartile	1.54	0.72–3.29	0.26	1.52	0.33–7.03	0.59	1.46	0.57–3.45	0.47
Trend test			0.23			0.78			0.28

[1]All risk estimates use lowest quartile as referent group.

Table 4. Effect modification of PhIP-DNA adduct level[1] associations with prostate cancer

	Whole sample ($n = 534$ case–control pairs)			African Americans ($n = 213$ case–control pairs)			Whites ($n = 321$ case–control pairs)		
Effect Modifier	**OR**	**95% CI**	***p* value**	**OR**	**95% CI**	***p* value**	**OR**	**95% CI**	***p* value**
PSA at cohort entry									
PSA < 4 ng mL/Low PhIP	1			1			1		
PSA < 4 ng mL/High PhIP	1.35	0.79–2.32	0.27	0.89	0.35–2.27	0.81	1.63	0.84–3.18	0.15
PSA ≥ 4 ng mL/Low PhIP	3.39	2.14–5.36	<0.0001	3.73	1.83–7.62	0.0003	3.08	1.69–5.63	0.0002
PSA ≥ 4 ng mL/High PhIP	3.21	2.00–5.15	<0.0001	2.37	1.08–5.19	0.03	3.62	1.99–6.58	<0.0001
PSA ≥ 4 ng mL ×									
High PhIP interaction	0.70	0.39–1.27	0.24	0.71	0.26–1.93	0.51	0.72	0.34–1.52	0.39
Glandular inflammation									
No Inflammation/Low PhIP	1			1			1		
No Inflammation/High PhIP	1.06	0.75–1.48	0.75	0.70	0.40–1.25	0.23	1.29	0.84–1.96	0.25
Inflammation/Low PhIP	0.78	0.48–1.27	0.32	1.01	0.49–2.07	0.98	0.64	0.32–1.26	0.20
Inflammation/High PhIP	1.54	0.91–2.61	0.11	1.56	0.54–4.52	0.42	1.61	0.87–2.99	0.13
Inflammation ×									
High PhIP interaction	1.87	0.95–3.68	0.07	2.19	0.65–7.43	0.21	1.97	0.83–4.69	0.13
HGPIN									
No HGPIN/Low PhIP	1			1			1		
No HGPIN/High PhIP	1.16	0.84–1.61	0.37	0.82	0.47–1.44	0.48	1.38	0.92–2.07	0.12
HGPIN/Low PhIP	2.16	1.07–4.37	0.03	2.88	1.04–7.98	0.04	1.52	0.55–4.16	0.42
HGPIN/High PhIP	2.25	1.12–4.51	0.02	0.79	0.24–2.59	0.69	3.89	1.56–9.73	0.004
HGPIN × High PhIP interaction	0.90	0.35–2.28	0.82	0.33	0.08–1.46	0.15	1.86	0.50–6.88	0.35
Partial Atrophy									
No atrophy/Low PhIP	1			1			1		
No atrophy/High PhIP	1.23	0.87–1.74	0.25	0.85	0.47–1.53	0.58	1.48	0.95–2.30	0.08
Atrophy/Low PhIP	0.98	0.66–1.46	0.92	1.12	0.62–2.02	0.72	0.89	0.51–1.54	0.67
Atrophy/High PhIP	1.00	0.66–1.74	1.00	0.59	0.27–1.28	0.18	1.25	0.76–2.08	0.38
Atrophy × High PhIP interaction	0.83	0.49–1.41	0.49	0.63	0.26–1.52	0.30	0.95	0.48–1.89	0.89

[1]High PhIP was considered above median level in controls.

time to diagnosis among White cases (supporting information Figure 2). While cases with elevated adduct levels were diagnosed more rapidly within 2–3 years of follow-up, the greatest difference in risk between the lowest and highest quartiles was observed 5–7 years after cohort entry. Overall, the four quartile curves for time to diagnosis were significantly different (log rank p-value = 0.05).

We next tested whether known clinical or histological prostate cancer risk factors modified the relationship between elevated PhIP-DNA adduct levels and prostate cancer (Table 4). Overall, no factors significantly modified the risk associated with elevated adduct levels and prostate cancer, although some interesting trends emerged. Partial atrophy and glandular inflammation were both associated with PhIP-DNA adducts in this study population in a race-specific manner, but neither modified the risk of prostate cancer associated with high adduct levels. Glandular inflammation had the highest interaction OR (OR = 2.19 in African Americans; 1.97 in Whites), and although neither OR was statistically significant, it appeared that elevated PhIP-DNA adduct levels increased risk for prostate cancer only in the presence of glandular inflammation. HGPIN was associated with prostate cancer in this study population,[24] and it modestly enhanced the association between elevated adduct levels and prostate cancer in Whites. In the absence of HGPIN, elevated PhIP-DNA adducts increased the risk for prostate cancer by 38%, but in the presence of both HGPIN and high PhIP-DNA adducts level, the risk increased almost four-fold (OR = 3.89; CI = 1.56–9.73). This is in contrast to what was observed in African Americans where the combination of HGPIN and elevated PhIP-DNA adduct levels actually decreased prostate cancer risk.

Discussion

We report for the first time a prospective analysis of PhIP-DNA adduct levels—a marker of biologically effective exposure to PhIP—measured in histopathologically benign tissue, and subsequent cancer risk for the same organ. Prior prospective studies of adduct levels and cancer risk have used surrogate tissues, such as white blood cells, but the correlation between adduct levels in these surrogate tissues *versus* the target organ is unclear.[33,34] Here we find that higher levels of PhIP-DNA adducts in benign prostate specimens were associated with a modestly increased risk for prostate cancer in White men. When the analysis was restricted to White cases diagnosed more than 4 years after tissue collection, however, patients with the highest PhIP-DNA adduct levels had almost three-fold increased risk of prostate cancer. In African Americans, we did not detect any observable increased risk associated with high PhIP-DNA adduct levels, in either the full sample or subgroups.

Until now, the question of whether PhIP increases risk for prostate cancer has largely been addressed using estimated dietary consumption of PhIP.[35] The first such effort found no increased risk of prostate cancer with increasing PhIP consumption.[36] A subsequent prospective study found a modest 22% increased prostate cancer risk for the highest PhIP consumption, with a statistically significant trend.[21] Since that study, multiple cohort[17,18,20] and case-control[16,19] questionnaire-based studies have been performed, collectively providing equivocal results concerning dietary PhIP consumption and prostate cancer risk. Given the high potential for measurement error using questionnaire data, biomarker studies are needed to address the potential carcinogenicity of this compound.

Despite availability of an anti-PhIP-DNA adduct antibody for immunohistochemistry studies,[12,22,25], only two case-control studies of cancer have employed this method previously; both finding higher PhIP-DNA adduct levels in benign tissue of the cancer-affected organ of cases compared with the corresponding tissue of controls.[22,23] Adduct levels were four times more likely to be high in benign tissue of breast cancer cases than controls[22] and 3.5 times more likely to be high in benign tissue of pancreatic cancer cases than controls.[23] To date, ours is the first such study to be performed in human prostate and the only study of PhIP-DNA adduct levels in pre-disease tissue.

Our previous study of men with prostate cancer found no racial differences in PhIP adduct levels in prostate tissue,[13] but in this study, we found that Whites had significantly higher levels of PhIP adducts in benign prostate than African Americans. Dietary data strongly suggest African Americans have higher exposure to PhIP through food preparation methods that differ by race[28] and African Americans have been shown to excrete more PhIP in urine.[30] Both activation and detoxification of PhIP play a role in adduct formation. African American men have slightly higher activity levels of the PhIP-metabolizing enzyme SULT1A1 than Whites.[29] However, both African Americans and Whites show an association between prostate cancer risk, SULT1A1 levels, and the Arg213His functional polymorphism in the *SULT1A1* gene.[29] African Americans also have higher enzymatic activity levels of CYP1A2 and N-acetyltransferase,[37] two enzymes important in the O-acetylation and N-oxidation of PhIP, respectively. PhIP and its carcinogenic metabolite N-hydroxy-PhIP (N-OH-PhIP) are extensively conjugated by UDP-glucuronosyltransferases (UGTs),[9] and UGT1A1 is the predominant UGT involved in PhIP metabolism[38]; notably, the most prevalent *UGT1A1* genotype in African Americans is associated with a lower capacity to detoxify PhIP.[39] While PhIP detoxification by UGT1A1 appears to be less efficient in African Americans, a study of *UGT1A1* genetic variation and colon cancer risk found an elevated risk associated with intermediate- to low-activity *UGT1A1* genotypes in Whites but not in African Americans.[40] This is consistent with our recent study that found non-specific genetic variation related to African ancestry to be a stronger predictor of PhIP-DNA adduct levels in prostate tissue than genetic variation in either *UGT1A1* or *SULT1A1*.[11] While the literature reviewed above would suggest that African Americans should have higher PhIP-DNA adduct levels and subsequently a greater risk of cancer associated with this marker than Whites, our results suggest the opposite. Clearly the carcinogenic potential of PhIP in human prostate is more complex than the sum of what is currently known about race-specific dietary exposure and genetic variation in PhIP metabolism.[41,42]

Our findings may be better understood by considering the histological cofactors we found to be associated with adduct levels. Inflammation and atrophy are hypothesized to be precursors of prostate cancer.[43,44] Inflammatory cytokines are known to suppress the activity of CYP1A enzymes[45] which is expressed in human prostate tumor and normal cells[46,47]; experimental evidence has shown that human prostate cells can activate PhIP and incur subsequent downstream effects such as DNA adduct formation and damage.[8,48] We found that adduct levels were higher when partial atrophy was present, and that PhIP-DNA adducts and HGPIN may act synergistically to increase prostate cancer risk in White men. In both races, adduct levels were highest in cases with partial but no simple atrophy and prostate cancer risk was increased only in the presence of both high PhIP-DNA adduct levels and glandular inflammation. Based on these findings we propose the model described in Figure 2 as to how PhIP might increase prostate cancer risk in humans. This model assumes variation in inherited susceptibility to metabolize PhIP and other dietary cofactors. The state of the inflammatory environment within the PhIP-exposed prostate is potentially related to both the amount of PhIP-DNA adducts created and prostate cancer risk.

Our study was observational, and while the duration of at-risk follow-up was equal for cases and controls, cohort members differed in their medical follow-up and screening behavior. Cases had significantly more PSA tests between cohort entry and diagnosis than controls, and the frequency of PSA tests in our study sample was greater than current

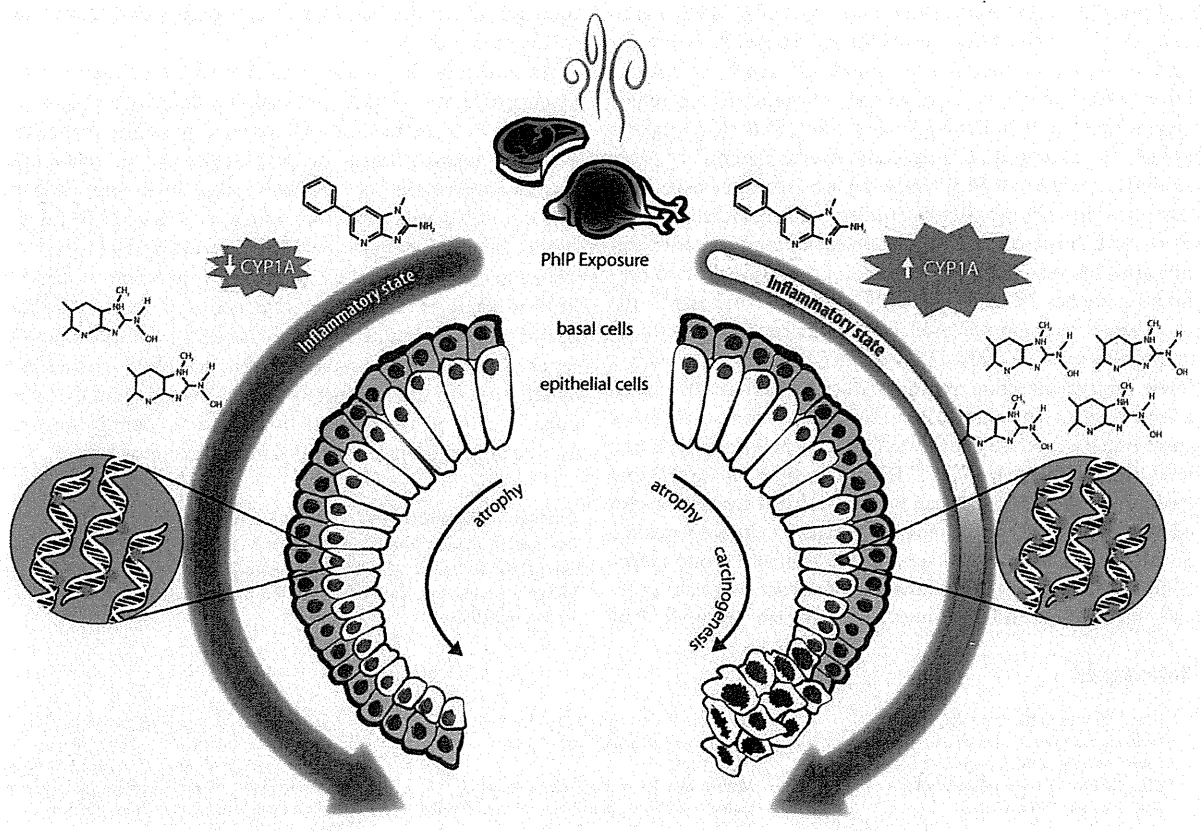

Figure 2. Proposed model of PhIP metabolism and DNA adduct formation in human prostate in relation to inflammation, atrophy and cancer risk. Depending on inherited susceptibility and level of dietary intake, PhIP exposure elicits a variable inflammatory response. A strong response (left side of figure) may dampen the expression of CYP1A enzymes, leading to accumulation of fewer active PhIP metabolites (N_2-hydroxy-PhIP), and subsequently lower levels of DNA adducts; a strong inflammatory response would also accelerate atrophy of prostate glandular cells, but not necessarily lead to carcinogenesis. Alternatively, a weak inflammatory response to PhIP exposure (right side of figure) may result in higher CYP1A activity levels, generation of more active PhIP metabolites, and subsequently higher levels of DNA adducts, but the progression of cellular atrophy would not be as rapid. A late elevated inflammatory response coupled with high levels of DNA adducts could incite prostate carcinogenesis. [Color figure can be viewed in the online issue, which is available at wileyonlinelibrary.com]

screening recommendations, even in controls. However, there is no *a priori* reason why screening behavior should differ by adduct levels and, indeed, adjustment for number of PSA tests during follow-up did not substantively change our results. While we were able to analyze 93% of eligible pairs, included pairs were slightly over-represented by younger cases and newer tissue samples, which tended to show stronger associations between PhIP-DNA adduct levels and prostate cancer risk in Whites. Based on the age range of our cohort and the high prevalence of undiagnosed prostate cancer in older men,[49] some men in our cohort likely had synchronous prostate cancer that was missed on initial biopsy. One would expect these cohort members misclassified as "disease-free" to be diagnosed sooner[50] and bias risk estimates toward the null. Hence risk estimates in men with longer follow-up may be less biased—suggesting that the greater prostate cancer risk associated with high PhIP-DNA adduct levels we observed in White men with four or more years of follow-up is closer to the true risk estimate.

In using a semi-quantitative immunohistochemical assay to measure PhIP-DNA adduct levels, our results are subject to several limitations. The specificity of the antibody we used to detect PhIP-DNA adducts has not been validated against the full range of possible mutagenic HCAs generated in well-done meats; most notably, we were unable to test whether the antibody could distinguish between PhIP-DNA and 2-amino-3,4,8-dimethylimidazo[4,5-f]quinoxaline (DiMeIQx)-DNA adducts. Despite this, we believe our results remain valid for several reasons. Although several studies using food preparation questionnaire data suggest an increased prostate cancer risk associated with DiMeIQx intake,[16,17] to our knowledge, laboratory studies have not detected DiMeIQx-DNA adducts in prostate tissue. Furthermore, we have previously reported a dose–response relationship between grilled red meat intake

and prostate tissue levels of the same PhIP-DNA adduct antibody used in this study[12] even though DiMeIQx is present only in trace amounts in beef products.[53] Levels of PhIP in other cooked meats are also generally an order of magnitude greater than levels of DiMeIQx; as a result, DiMeIQx intake is unlikely to confound PhIP exposure measurements.[51,52] More sensitive methods of PhIP-DNA adduct detection have been attempted in only two human studies; neither studied prostate tissue, and the percentage of "undetectable" samples varied significantly between them.[54,55] Based on previously reported calibration studies of the PhIP-DNA adduct antibody,[22] the absorbency measure we used can detect roughly a 100-fold range difference in PhIP-DNA adduct concentration, with a lower limit of detection around $1/10^7$ nucleotides. While such a level might seem unrealistic in humans, a study using mass spectrometry detected PhIP-DNA adducts in lymphocytes at a level of 3×10^8 nucleotides.[55] Finally, because our study categorized the adduct data, it can be assumed that specimens with adduct levels undetectable by more sensitive methods would be in the lowest category, and serve as the reference group in statistical analyses. In addition, analysis of adduct data as categorical variables defined around the median ensured that measurement inaccuracies at the extremes would not over influence the results.

In summary, the increased risk of prostate cancer conferred by elevated levels of PhIP-DNA adducts in benign prostate tissue appears to be modest and confined to White men. However, the apparent dose–response nature of this relationship and its amplification in men with longer follow-up lends credence to this result. Based on animal models of PhIP-induced carcinogenesis, synergies between elevated adduct levels and pre-neoplastic changes are biologically plausible. Clearly, if PhIP is acting as a prostate carcinogen in humans, significant risk of cancer from PhIP exposure is likely confined to the subset of men with greater capacity to activate PhIP. Further study of determinates of PhIP metabolism in humans, and the role of inflammation in this process, is needed to identify men that may be at greatest risk for PhIP-induced carcinogenesis.

Acknowledgements

The authors thank the medical record abstractors and other study personnel that helped with data collection for this study. The authors especially thank Travis Wheeler and Nancy Lemke who processed all prostate specimens used in this study.

References

1. Felton JS, Knize MG, Shen NH, et al. The isolation and identification of a new mutagen from fried ground beef: 2-amino-1-methyl-6-phenylimidazo[4,5-b]pyridine (PhIP). *Carcinogenesis* 1986;7:1081–6.
2. Shirai T, Sano M, Tamano S, et al. The prostate: a target for carcinogenicity of 2-amino-1-methyl-6-phenylimidazo[4,5-b]pyridine (PhIP) derived from cooked foods. *Cancer Res* 1997;57:195–8.
3. Nakai Y, Nelson WG, De Marzo AM. The dietary charred meat carcinogen 2-amino-1-methyl-6-phenylimidazo[4,5-b]pyridine acts as both a tumor initiator and promoter in the rat ventral prostate. *Cancer Res* 2007;67:1378–84.
4. Shirai T, Kato K, Futakuchi M, et al. Organ differences in the enhancing potential of 2-amino-1-methyl-6-phenylimidazo[4,5-b]pyridine on carcinogenicity in the prostate, colon and pancreas. *Mutat Res* 2002;506–507:129–36.
5. Cui L, Takahashi S, Tada M, et al. Immunohistochemical detection of carcinogen-DNA adducts in normal human prostate tissues transplanted into the subcutis of athymic nude mice: results with 2-amino-1-methyl-6-phenylimidazo[4,5-b]pyridine (PhIP) and 3,2'-dimethyl-4-aminobiphenyl (DMAB) and relation to cytochrome P450s and N-acetyltransferase activity. *Jpn J Cancer Res* 2000;91:52–8.
6. Li G, Wang H, Liu AB, et al. Dietary carcinogen 2-amino-1-methyl-6-phenylimidazo[4,5-b]pyridine-induced prostate carcinogenesis in CYP1A-humanized mice. *Cancer Prev Res* 2012;5:963–72.
7. Wang CY, Debiec-Rychter M, Schut HA, et al. N-Acetyltransferase expression and DNA binding of N-hydroxyheterocyclic amines in human prostate epithelium. *Carcinogenesis* 1999;20:1591–5.
8. Williams JA, Martin FL, Muir GH, et al. Metabolic activation of carcinogens and expression of various cytochromes P450 in human prostate tissue. *Carcinogenesis* 2000;21:1683–9.
9. Malfatti MA, Felton JS. N-glucuronidation of 2-amino-1-methyl-6-phenylimidazo[4,5-b]pyridine (PhIP) and N_hydroxy-PhIP by specific human UDP-glucuronosyltransferases. *Carcinogenesis* 2001;22:1087–93.
10. Di Paolo OA, Teitel CH, Nowell S, et al. Expression of cytochromes P450 and glutathione S-transferases in human prostate, and the potential for activation of heterocyclic amine carcinogens via acetyl-coA-. *Int J Cancer* 2005;117:8–13.
11. Rybicki BA, Neslund-Dudas C, Bock CH, et al. Red wine consumption is inversely associated with 2-amino-1-methyl-6-phenylimidazo[4,5-b]pyridine-DNA adduct levels in prostate. *Cancer Prev Res (Phila)* 2011;4:1636–44.
12. Tang D, Liu JJ, Rundle A, et al. Grilled meat consumption and PhIP-DNA adducts in prostate carcinogenesis. *Cancer Epidemiol Biomarkers Prev* 2007;16:803–8.
13. Tang D, Liu JJ, Bock CH, et al. Racial differences in clinical and pathological associations with PhIP-DNA adducts in prostate. *Int J Cancer* 2007;121:1319–24.
14. Kooiman GG, Martin FL, Williams JA, et al. The influence of dietary and environmental factors on prostate cancer risk. *Prostate Cancer Prostatic Dis* 2000;3:256–8.
15. El-Zein R, Etzel CJ, Lopez MS, et al. Human sensitivity to PhIP: a novel marker for prostate cancer risk. *Mutat Res* 2006;601:1–10.
16. Punnen S, Hardin J, Cheng I, et al. Impact of meat consumption, preparation, and mutagens on aggressive prostate cancer. *PLoS One* 2011;6:e27711.
17. Major JM, Cross AJ, Watters JL, et al. Patterns of meat intake and risk of prostate cancer among African-Americans in a large prospective study. *Cancer Causes Control* 2011;22:1691–8.
18. Koutros S, Cross AJ, Sandler DP, et al. Meat and meat mutagens and risk of prostate cancer in the Agricultural Health Study. *Cancer Epidemiol Biomarkers Prev* 2008;17:80–7.
19. John EM, Stern MC, Sinha R, et al. Meat consumption, cooking practices, meat mutagens, and risk of prostate cancer. *Nutr Cancer* 2011;63:525–37.
20. Sander A, Linseisen J, Rohrmann S. Intake of heterocyclic aromatic amines and the risk of prostate cancer in the EPIC-Heidelberg cohort. *Cancer Causes Control* 2011;22:109–14.
21. Cross AJ, Peters U, Kirsh VA, et al. A prospective study of meat and meat mutagens and prostate cancer risk. *Cancer Res* 2005;65:11779–84.
22. Zhu J, Chang P, Bondy ML, et al. Detection of 2-amino-1-methyl-6-phenylimidazo[4,5-b]-pyridine-DNA adducts in normal breast tissues and risk of breast cancer. *Cancer Epidemiol Biomarkers Prev* 2003;12:830–7.
23. Zhu J, Rashid A, Cleary K, et al. Detection of 2-amino-1-methyl-6-phenylimidazo [4,5-b]-pyridine (PhIP)-DNA adducts in human pancreatic tissues. *Biomarkers* 2006;11:319–28.
24. Kryvenko ON, Jankowski M, Chitale DA, et al. Inflammation and preneoplastic lesions in benign prostate as risk factors for prostate cancer. *Mod Pathol* 2012;25:1023–32.
25. Takahashi S, Tamano S, Hirose M, et al. Immunohistochemical demonstration of carcinogen-DNA adducts in tissues of rats given 2-amino-1-methyl-6-phenylimidazo[4,5-b]pyridine (PhIP): detection in paraffin-embedded sections and tissue distribution. *Cancer Res* 1998;58:4307–13.
26. Lin D, Kaderlik KR, Turesky RJ, et al. Identification of N-(Deoxyguanosin-8-yl)−2-

Epidemiology

amino-1-methyl-6-phenylimidazo [4,5-b]pyridine as the major adduct formed by the food-borne carcinogen, 2-amino-1-methyl-6-phenylimidazo[4,5-b]pyridine, with DNA. *Chem Res Toxicol* 1992;5:691–7.
27. Takahashi S, Hasegawa R, Mutai M, et al. Additive action of five heterocyclic amines in terms of induction of GST-P positive single cells and foci in rat liver-correlation with DNA adduct formation. *J Toxicol Pathol* 1994;7:423–8.
28. Bogen KT, Keating GA. U.S. dietary exposures to heterocyclic amines. *J Expo Anal Environ Epidemiol* 2001;11:155–68.
29. Nowell S, Ratnasinghe DL, Ambrosone CB, et al. Association of SULT1A1 phenotype and genotype with prostate cancer risk in African-Americans and Caucasians. *Cancer Epidemiol Biomarkers Prev* 2004;13:270–6.
30. Kidd LC, Stillwell WG, Yu MC, et al. Urinary excretion of 2-amino-1-methyl-6-phenylimidazo[4,5-b]pyridine (PhIP) in White, African-American, and Asian-American men in Los Angeles County. *Cancer Epidemiol Biomarkers Prev* 1999;8:439–45.
31. Kriek E, Rojas M, Alexandrov K, et al. Polycyclic aromatic hydrocarbon-DNA adducts in humans: relevance as biomarkers for exposure and cancer risk. *Mutat Res* 1998;400:215–31.
32. Gammon MD, Santella RM, Neugut AI, et al. Environmental toxins and breast cancer on Long Island. I. Polycyclic aromatic hydrocarbon DNA adducts. *Cancer Epidemiol Biomarkers Prev* 2002;11:677–85.
33. van Schooten FJ, Hillebrand MJ, van Leeuwen FE, et al. Polycyclic aromatic hydrocarbon—DNA adducts in white blood cells from lung cancer patients: no correlation with adduct levels in lung. *Carcinogenesis* 1992;13:987–93.
34. Wiencke JK, Kelsey KT, Varkonyi A, et al. Correlation of DNA adducts in blood mononuclear cells with tobacco carcinogen-induced damage in human lung. *Cancer Res* 1995;55:4910–4.
35. Sinha R. An epidemiologic approach to studying heterocyclic amines. *Mutat Res* 2002;506–507:197–204.
36. Norrish AE, Ferguson LR, Knize MG, et al. Heterocyclic amine content of cooked meat and risk of prostate cancer. *J Natl Cancer Inst* 1999;91:2038–44.
37. Relling MV, Lin JS, Ayers GD, et al. Racial and gender differences in N-acetyltransferase, xanthine oxidase, and CYP1A2 activities. *Clin Pharmacol Ther* 1992;52:643–58.
38. Malfatti MA, Felton JS. Human UDP-glucuronosyltransferase 1A1 is the primary enzyme responsible for the N-glucuronidation of N-hydroxy-PhIP in vitro. *Chem Res Toxicol* 2004;17:1137–44.
39. Girard H, Thibaudeau J, Court MH, et al. UGT1A1 polymorphisms are important determinants of dietary carcinogen detoxification in the liver. *Hepatology* 2005;42:448–57.
40. Girard H, Butler LM, Villeneuve L, et al. UGT1A1 and UGT1A9 functional variants, meat intake, and colon cancer, among Caucasians and African-Americans. *Mutat Res* 2008;644:56–63.
41. Knize MG, Kulp KS, Salmon CP, et al. Factors affecting human heterocyclic amine intake and the metabolism of PhIP. *Mutat Res* 2002;506–507:153–62.
42. Malfatti MA, Dingley KH, Nowell-Kadlubar S, et al. The urinary metabolite profile of the dietary carcinogen 2-amino-1-methyl-6-phenylimidazo[4,5-b]pyridine is predictive of colon DNA adducts after a low-dose exposure in humans. *Cancer Res* 2006;66:10541–7.
43. Wang W, Bergh A, Damber JE. Morphological transition of proliferative inflammatory atrophy to high-grade intraepithelial neoplasia and cancer in human prostate. *Prostate* 2009;69:1378–86.
44. Sfanos KS, De Marzo AM. Prostate cancer and inflammation: the evidence. *Histopathology* 2012;60:199–215.
45. Abdel-Razzak Z, Loyer P, Fautrel A, et al. Cytokines down-regulate expression of major cytochrome P-450 enzymes in adult human hepatocytes in primary culture. *Mol Pharmacol* 1993;44:707–15.
46. Sterling KM, Jr, Cutroneo KR. Constitutive and inducible expression of cytochromes P4501A (CYP1A1 and CYP1A2) in normal prostate and prostate cancer cells. *J Cell Biochem* 2004;91:423–9.
47. Murray GI, Taylor VE, McKay JA, et al. The immunohistochemical localization of drug-metabolizing enzymes in prostate cancer. *J Pathol* 1995;177:147–52.
48. Martin FL, Cole KJ, Muir GH, et al. Primary cultures of prostate cells and their ability to activate carcinogens. *Prostate Cancer Prostatic Dis* 2002;5:96–104.
49. Sakr WA, Grignon DJ, Crissman JD, et al. High grade prostatic intraepithelial neoplasia (HGPIN) and prostatic adenocarcinoma between the ages of 20–69: an autopsy study of 249 cases. *In Vivo* 1994;8:439–43.
50. Nonn L, Ananthanarayanan V, Gann PH. Evidence for field cancerization of the prostate. *Prostate* 2009;69:1470–9.
51. Keating GA, Bogen KT. Estimates of heterocyclic amine intake in the US population. *J Chromatogr B Analyt Technol Biomed Life Sci* 2004;802:127–33.
52. Keating GA, Bogen KT. Methods for estimating heterocyclic amine concentrations in cooked meats in the US diet. *Food Chem Toxicol* 2001;39:29–43.
53. Sinha R, Rothman N, Salmon CP, et al. Heterocyclic amine content in beef cooked by different methods to varying degrees of doneness and gravy made from meat drippings. *Food Chem Toxicol* 1998;36:279–87.
54. Gu D, Turesky RJ, Tao Y, et al. DNA adducts of 2-amino-1-methyl-6-phenylimidazo[4,5-b]pyridine and 4-aminobiphenyl are infrequently detected in human mammary tissue by liquid chromatography/tandem mass spectrometry. *Carcinogenesis* 2012;33:124–30.
55. Magagnotti C, Pastorelli R, Pozzi S, et al. Genetic polymorphisms and modulation of 2-amino-1-methyl-6-phenylimidazo[4,5-b]pyridine (PhIP)-DNA adducts in human lymphocytes. *Int J Cancer* 2003;107:878–84.

Diabetologia (2012) 55:1745–1754
DOI 10.1007/s00125-012-2521-5

ARTICLE

Control of beta cell function and proliferation in mice stimulated by small-molecule glucokinase activator under various conditions

A. Nakamura · Y. Togashi · K. Orime · K. Sato · J. Shirakawa · M. Ohsugi · N. Kubota · T. Kadowaki · Y. Terauchi

Received: 14 November 2011 / Accepted: 20 February 2012 / Published online: 29 March 2012

Abstract
Aims/hypothesis We investigated changes in the expression of genes involved in beta cell function and proliferation in mouse islets stimulated with glucokinase activator (GKA) in order to elucidate the mechanisms by which GKA stimulates beta cell function and proliferation.
Methods Islets isolated from mice were used to investigate changes in the expression of genes related to beta cell function and proliferation stimulated by GKA. In addition, *Irs2* knockout (*Irs2*$^{-/-}$) mice on a high-fat diet or a high-fat diet containing GKA were used to investigate the effects of GKA on beta cell proliferation in vivo.
Results In wild-type mice, *Irs2* and *Pdx1* expression was increased by GKA. In *Irs2*$^{-/-}$ mice, GKA administration increased the glucose-stimulated secretion of insulin and *Pdx1* expression, but not beta cell proliferation. It was particularly noteworthy that oxidative stress inhibited the upregulation of the *Irs2* and *Pdx1* genes induced by GKA. Moreover, whereas neither GKA alone nor exendin-4 alone upregulated the expression of *Irs2* and *Pdx1* in the islets of *db/db* mice, prior administration of exendin-4 to the mice caused GKA to increase the expression of these genes.
Conclusions/interpretation GKA-stimulated IRS2 production affected beta cell proliferation but not beta cell function. Oxidative stress diminished the effects of GKA on the changes in expression of genes involved in beta cell function and proliferation. A combination of GKA and an incretin-related agent might therefore be effective in therapy.

Keywords Beta cell proliferation · Glucokinase activator · IRS2 · Oxidative stress

Abbreviations

CREB	cAMP-responsive element-binding protein
2-DG	2-Deoxyglucose
GKA	Glucokinase activator
HF	High-fat

Introduction

Glucokinase is the predominant enzyme involved in glucose phosphorylation in beta cells and hepatocytes, and it plays an important role as a glucose sensor in beta cells and as a regulator of glucose metabolism in the liver [1, 2]. In addition, glucokinase plays a pivotal role in regulating not only beta cell function, but also beta cell mass [3, 4].

Since the report by Grimsby et al in 2003 [5], several glucokinase activators (GKAs) have been developed, and these have been shown to lower blood glucose in several animal models of type 2 diabetes [5–12]. In a study of beta cell function, it was reported that a GKA stimulated insulin secretion in a Ca^{2+}-dependent manner in rodent islets and MIN6 cells [13], and we and others have reported that GKAs promoted beta cell proliferation and increased production of IRS2 [11, 14], which is critically required for beta

A. Nakamura · Y. Togashi · K. Orime · K. Sato · J. Shirakawa · Y. Terauchi (✉)
Department of Endocrinology and Metabolism, Graduate School of Medicine, Yokohama City University, 3-9 Fukuura, Kanazawa-ku, Yokohama 236-0004, Japan
e-mail: terauchi-tky@umin.ac.jp

M. Ohsugi · N. Kubota · T. Kadowaki
Department of Diabetes and Metabolic Diseases, Graduate School of Medicine, University of Tokyo, Tokyo, Japan

cell growth and survival [3, 15–17]. However, the exact mechanisms by which GKAs stimulate beta cell function and proliferation are largely unknown.

Single- and multiple-dose placebo-controlled studies in human have recently reported that GKAs reduce the fasting and postprandial glucose levels of patients with type 2 diabetes and of healthy adults [18, 19]. Notably, however, another GKA, MK-0941, led to improvements in glycaemic control that were not sustained [20]. Therefore, a better understanding of the underlying mechanism is needed to determine whether glucokinase activation with GKAs is a feasible treatment goal for individuals with type 2 diabetes.

In the present study, we first investigated changes in the expression of genes involved in beta cell function and proliferation in mouse islets stimulated with GKA in order to elucidate the mechanisms by which GKA stimulated beta cell function and proliferation. We then explored therapeutic strategies by which GKA might work more effectively.

Methods

Chemicals A GKA (3-[(1*S*)-2-hydroxy-1-methylethoxy]-5-[4-(methylsulfonyl)phenoxy]-*N*-1,3-thiazol-2-yl benzamide) was prepared by Tsukuba Research Institute, Banyu Pharmaceutical, Tokyo, Japan, as previously described [21].

Animals *Irs2*$^{-/-}$ mice were generated as described elsewhere [16] and were then backcrossed with C57Bl/6J mice more than nine times. Both wild-type and *Irs2*$^{-/-}$ male mice were fed standard chow until 8 weeks of age, when they were given free access to either the standard chow, a high-fat (HF) diet, or an HF diet containing GKA. To evaluate the effect of GKA on glucose metabolism in vivo more thoroughly, wild-type and *Irs2*$^{-/-}$ mice were divided into four groups: wild-type mice fed the HF diet, wild-type mice fed the HF diet containing 0.04% GKA, *Irs2*$^{-/-}$ mice fed the HF diet, and *Irs2*$^{-/-}$ mice fed the HF diet containing 0.04% GKA. Five-week-old male *db/db* mice were purchased from Charles River Laboratories Japan (Yokohama, Japan). When they were 6 weeks of age, they were intraperitoneally injected with normal saline or exendin-4 (100 μg/kg; Sigma-Aldrich, Tokyo, Japan) once daily for 2 weeks. The mice were housed under a 12-h light/dark cycle. The animals were maintained in accordance with standard animal care procedures based on the institutional guidelines.

Diet protocol Standard chow (MF; Oriental Yeast, Tokyo, Japan) and an HF diet (High Fat Diet 32; Clea Japan, Tokyo, Japan) were used. GKA was administrated in the form of a 0.04% (wt/wt) admixture to the HF diet as previously described [11].

Glucose tolerance test Mice were fasted for 4 h before the study, and then orally loaded with a 1.5 mg/g body weight dose of glucose. Blood glucose was measured with a Glutest Neo portable glucose meter (Sanwa Chemical, Nagoya, Japan).

Immunohistochemical analysis to estimate beta cell mass Isolated pancreases were immersion-fixed in 10% formalin at 4°C overnight. Tissue was then routinely processed for paraffin embedding, and 5 μm sections mounted on glass slides were immunostained with rabbit anti-human insulin (diluted 1:1,000) antibody (Santa Cruz Biotechnology, Santa Cruz, CA, USA). The area of the beta cells was calculated with WinROOF software (Mitani, Tokyo, Japan) as described elsewhere [3]. Approximately 100 islets per mouse were counted in each group.

Analysis of BrdU incorporation Wild-type and *Irs2*$^{-/-}$ mice on the HF diet for 10 weeks were divided into two groups: an HF diet group, and a group given 0.04% GKA mixed into the HF diet. After 3 days, the mice were intraperitoneally injected with BrdU (Nacalai Tesque, Kyoto, Japan), and the pancreases were removed 6 h later. Immunohistochemical detection of BrdU was performed with a commercial kit (BD Biosciences, Franklin Lakes, NJ, USA). Approximately 100 islets per mouse were counted in each group.

Islet isolation Islets were isolated by using liberase RI (Roche Diagnostics, Indianapolis, IN, USA) or collagenase XI (Sigma-Aldrich, St Louis, MO, USA) according to the manufacturer's instructions, as described elsewhere [3, 11].

Analysis of insulin secretion Insulin secretion was measured after culturing islets overnight in RPMI 1640 medium containing 11 mmol/l glucose supplemented with 10% fetal calf serum, 100 U/ml penicillin and 100 μg/ml streptomycin (Sigma-Aldrich, St Louis, MO, USA). Ten islets were incubated at 37°C for 1.5 h in Krebs–Ringer bicarbonate buffer containing 5.6 or 22 mmol/l glucose in the absence or presence of GKA. The insulin concentration of the assay buffer was measured with an insulin ELISA kit (Morinaga, Yokohama, Japan).

Real-time quantitative PCR Total RNA was isolated with the RNeasy Mini Kit (Qiagen, Hilden, Germany) and used as the starting material for complementary DNA (cDNA) preparation. cDNA was synthesised by using TaqMan Reverse Transcription Reagents (Applied Biosystems, Foster City, CA, USA), and TaqMan quantitative PCR was performed with the ABI Prism 7500 PCR instrument (Applied Biosystems).

Western blot analysis The anti-phospho [Ser133] cAMP-responsive element-binding protein (CREB), total CREB,

and cyclin D2 antibody were purchased from Cell Signaling Technology (Beverly, MA, USA). Anti-IRS2 antibody was purchased from Upstate (Temecula, CA, USA). Protein was prepared from more than 100 islets pooled from several mice in the same group, and 20 μg of protein samples were applied to the gel. Protein bands were visualised with the ECL Plus Western Blotting Detection System (GE Healthcare, Amersham, UK).

Statistical analysis Results are expressed as mean ± SE (n). Differences between two groups were analysed for statistical significance by Student's t test. Individual comparisons between more than two groups were assessed by the post hoc Fisher's PLSD test. A p value <0.05 was considered statistically significant.

Results

Mechanism of the upregulation of Irs2 expression in response to GKA-induced glucokinase activation Because we had hypothesised that glucose metabolism via glucokinase would increase the phosphorylation of CREB and the production of IRS2 [3, 22], we investigated whether the GKA was able to stimulate the phosphorylation of CREB. Ser133 phosphorylation of CREB was significantly increased at 22 mmol/l glucose in comparison with 5.6 mmol/l glucose, and the GKA stimulated the Ser133 phosphorylation of CREB in the isolated islets of wild-type mice at 5.6 mmol/l glucose (Fig. 1a). The phosphorylation of CREB paralleled the upregulation of IRS2 production.

As it has been reported that glucose treatment of isolated islets potently increases *Irs2* expression via glucose metabolism and Ca^{2+} influx [23], we examined changes in *Irs2* mRNA levels in response to GKA administration or high-glucose stimulation under several conditions to identify the mechanism of *Irs2* upregulation. First, we evaluated *Irs2* mRNA expression in response to the GKA and sulfonylureas. Real-time quantitative PCR showed that *Irs2* mRNA was significantly increased with 22 mmol/l glucose in comparison with 5.6 mmol/l glucose (Fig. 1c). The GKA also significantly increased *Irs2* mRNA with 5.6 mmol/l glucose, but neither gliclazide nor glibenclamide upregulated the *Irs2* mRNA level (Fig. 1c).

Next, we used the non-metabolisable analogue of glucose, 2-deoxyglucose (2-DG), to investigate whether glucose metabolism was required for GKA-stimulated *Irs2* expression. When glucose was replaced by 2-DG, the *Irs2* mRNA levels did not increase in response to the GKA or a stimulatory concentration of 2-DG (22 mmol/l; Fig. 1d), indicating that glucose metabolism is necessary for GKA-induced *Irs2* expression to occur in islet beta cells.

We also conducted experiments using an L-type calcium channel blocker (nifedipine) and calcineurin inhibitor

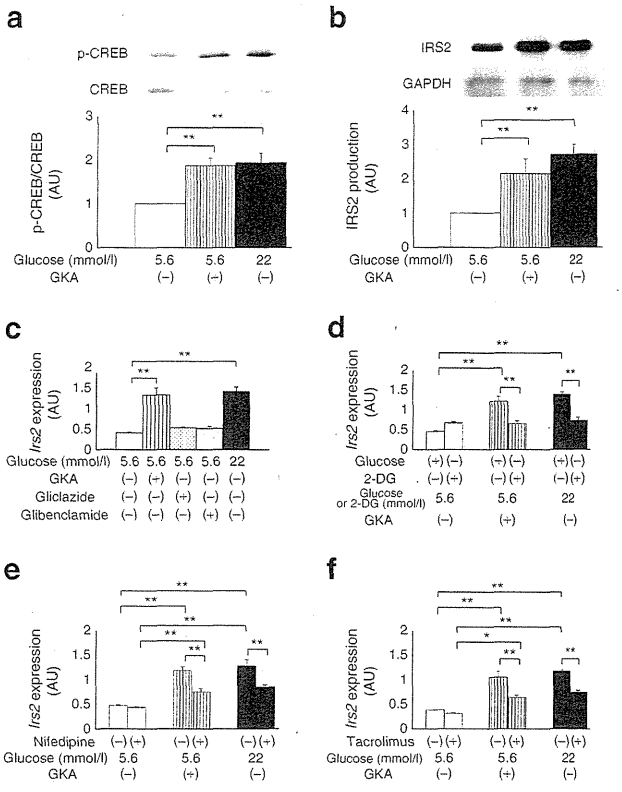

Fig. 1 Effect of GKA on upregulation of *Irs2* expression. **a** Western blot assay of phospho [Ser133] CREB (p-CREB) and total CREB levels in islets. **b** Production of IRS2 in islets. Islets from wild-type mice were stimulated with 5.6 mmol/l glucose in the absence or presence of 6 μmol/l GKA or with 22 mmol/l glucose alone. Equal amounts of lysates were blotted with the p-CREB, total CREB, IRS2 and GAPDH antibody. Expression levels were quantified. The intensity of p-CREB was normalised to total CREB expression, and the intensity of IRS2 was normalised to GAPDH expression (white bar, 5.6 mmol/l glucose; hatched bar, 5.6 mmol/l glucose plus GKA; black bar, 22 mmol/l glucose) (n=5). **c**–**f** Effects of (**c**) sulfonylureas (10 μmol/l gliclazide and 1 nmol/l glibenclamide), (**d**) 2-deoxyglucose (DG), (**e**) 50 μmol/l nifedipine, and (**f**) 10 μmol/l tacrolimus on *Irs2* expression. The *Irs2* and beta-actin (control) mRNA levels of isolated islets in wild-type mice were measured by real-time quantitative PCR. Data have been normalised to beta-actin expression (white bars, 5.6 mmol/l glucose; hatched bars, 5.6 mmol/l glucose plus GKA; dotted bars, 5.6 mmol/l glucose plus gliclazide; grey bar, 5.6 mmol/l glucose plus glibenclamide; black bars, 22 mmol/l glucose) (n=3 or 4). Values are mean ± SE. *p<0.05; **p<0.01

(tacrolimus). The results showed that both nifedipine (50 μM) and tacrolimus (10 μM) significantly inhibited the upregulation of *Irs2* mRNA levels induced by GKA administration or high-glucose stimulation, although the *Irs2* mRNA levels remained slightly but significantly increased (Fig. 1e, f). These results indicated that the GKA-induced *Irs2* upregulation in islets is at least partly Ca^{2+}-dependent and mediated by calcineurin.

Effect of the GKA on changes in gene expression in isolated islets Next, we investigated changes in the expression levels of genes involved in beta cell function and proliferation in the

islets of wild-type mice in the absence or presence of the GKA. *Pdx1* is the major regulator of glucose-stimulated insulin gene transcription, and its mRNA level was significantly increased at 22 mmol/l glucose in comparison with 5.6 mmol/l glucose; in addition, the GKA stimulated *Pdx1* mRNA production with 5.6 mmol/l glucose in the isolated islets of wild-type mice (Fig. 2a). The increased *Pdx1* levels paralleled the upregulation of *Glut2*, *Gck*, *Ins1* and *Ins2* expression (Fig. 2a). Gliclazide, however, failed to increase the expression levels of these (Fig. 2b). These results indicated that the GKA improved beta cell function at the transcriptional level.

As the results of a DNA microarray analysis we previously reported showed decreased expression of *Pdpk1* and *Ccnd2* in $Gck^{+/-}$ mice in comparison with wild-type mice on the HF diet [3], we investigated the expression levels of these and other cell-cycle-related genes in the present study. GKA and high-glucose stimulation significantly increased *Pdpk1*, *Ccnd1*, *Ccnd2* and *Ccnd3* mRNA expression, but the expression of *Cdk4* and p27 was unaltered (Fig. 2c). Cyclin D2 protein levels were also increased by the GKA and high-glucose stimulation (Fig. 2d). These results suggested an involvement of cell cycle signalling, such as by cyclin D2, in GKA-stimulated beta cell proliferation.

Effect of the GKA on glucose metabolism and beta cell mass in $Irs2^{-/-}$ mice We used $Irs2^{-/-}$ mice to determine whether IRS2 was required for the therapeutic effects of the GKA, and divided the animals into four groups: wild-type mice fed the HF diet (WT group), wild-type mice fed a diet containing 0.04 % GKA mixed into the HF diet (WT+GKA group). $Irs2^{-/-}$ mice fed the HF diet (IRS2 group), and $Irs2^{-/-}$ mice fed 0.04% GKA mixed into the HF diet (IRS2+GKA group).

There were no significant differences in body weight between mice receiving and mice not receiving GKA in both the wild-type and $Irs2^{-/-}$ groups (Fig. 3a). The blood glucose level decreased shortly after consuming the HF diet containing the GKA. The blood glucose level of the WT+GKA group was significantly lower than that of the WT group, and the blood glucose level of the IRS2+GKA group was significantly lower than that of the IRS2 group (Fig. 3b). We also performed an OGTT on these four groups of mice (Fig. 3c). The area under the curve (0–120 min) of the blood glucose levels during the OGTT was significantly decreased in both the wild-type and $Irs2^{-/-}$ mice that received the GKA compared with the mice that did not receive the GKA (Fig. 3d). Thus, GKA demonstrated glucose-lowering efficacy without affecting body weight in both the wild-type and $Irs2^{-/-}$ mice on the HF diet.

Next, to investigate the effect of GKA on beta cell mass, we measured the beta cell mass of the mice. Histological analysis revealed that the area of the beta cells was significantly increased in the wild-type mice in comparison with the $Irs2^{-/-}$ mice (Fig. 3e), consistent with our previous report [3], but no further increase was observed in response to administering GKA to either genotype of mouse (Fig. 3e).

As we previously reported [11], the absence of any effect of the GKA on the beta cell mass of the $Irs2^{-/-}$ mice may be attributable to a suppression of beta cell proliferation due to

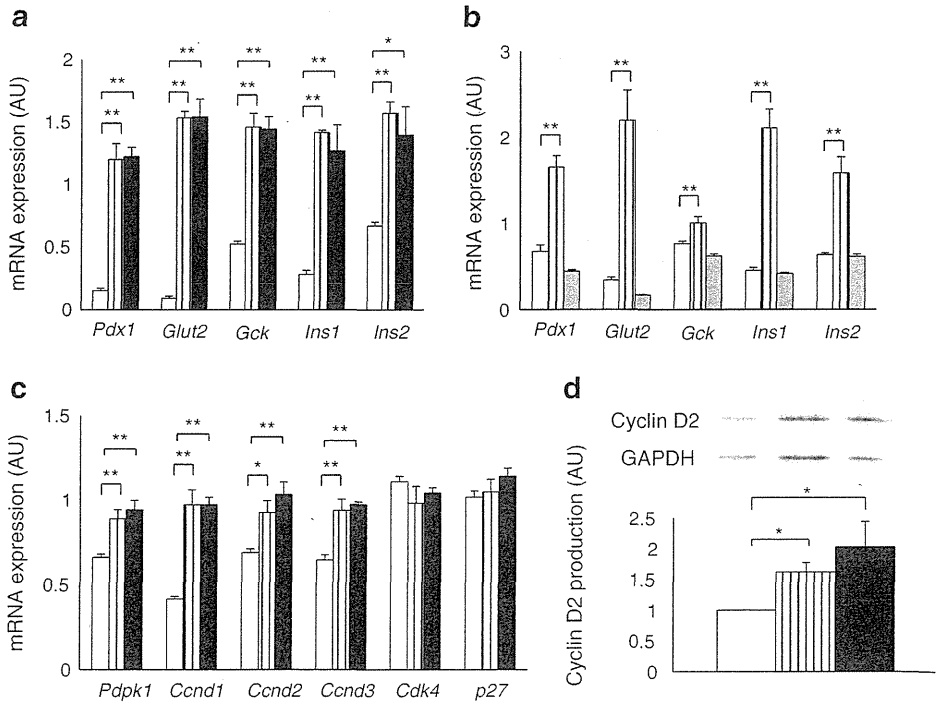

Fig. 2 Changes in gene expression levels in islets stimulated with GKA. **a–c** The mRNA levels of (**a, b**) *Pdx1*, *Glut2*, *Gck*, *Ins1* and *Ins2*, and of (**c**) *Pdpk1*, *Ccnd1*, *Ccnd2*, *Ccnd3*, *Cdk4* and *p27* in islets measured by real-time quantitative PCR. Data have been normalised to beta-actin expression. **d** Western blot assay of cyclin D2 levels in islets. Equal amounts of lysates were blotted with the cyclin D2 antibody and GAPDH antibody. Protein levels were quantified, and the cyclin D2 data have been normalised to GAPDH expression (white bars, 5.6 mmol/l glucose; hatched bars, 5.6 mmol/l glucose plus GKA; grey bars, 5.6 mmol/l glucose plus gliclazide; black bars, 22 mmol/l glucose) (n=3–5). Values are mean ± SE. *p<0.05; **p<0.01

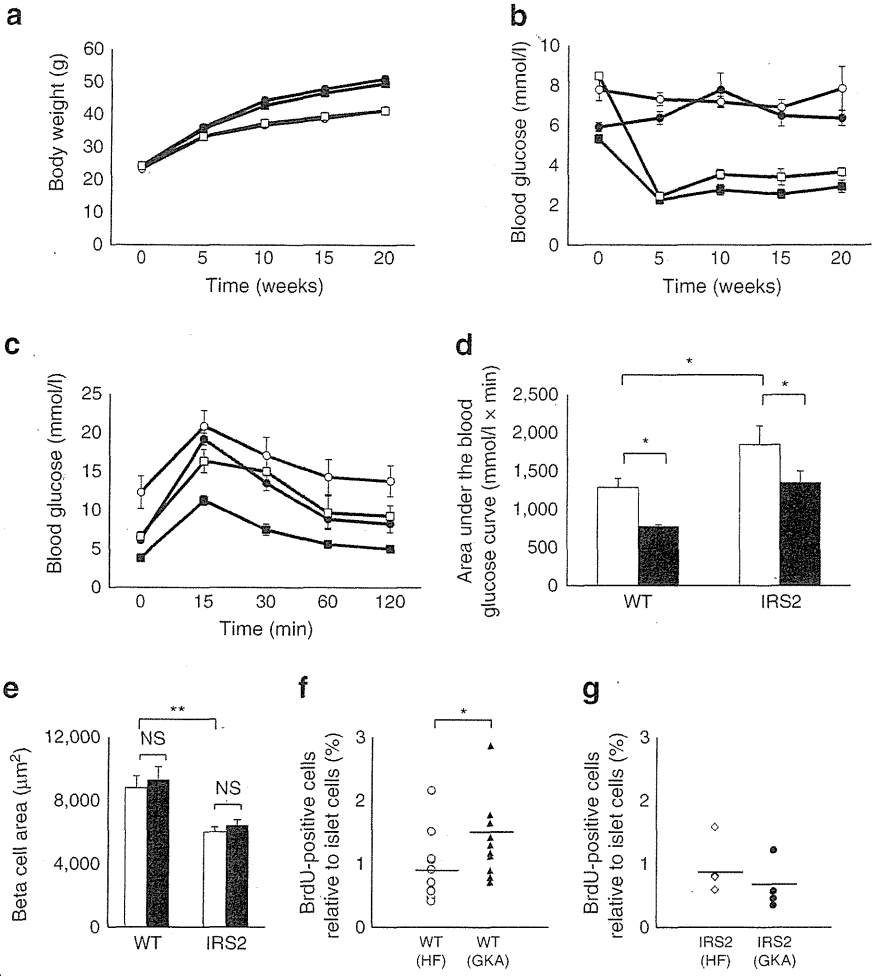

Fig. 3 Impact of GKA on glucose metabolism and on beta cell mass and proliferation in *Irs2*$^{-/-}$ mice. **a, b** Changes in (**a**) body weight and (**b**) fed blood glucose level. Wild-type mice on the HF diet (WT; black circles), wild-type mice fed the 0.04% GKA HF diet (WT+GKA; black squares), *Irs2*$^{-/-}$ mice fed the HF diet (IRS2; white circles) and *Irs2*$^{-/-}$ mice fed the 0.04% GKA HF diet (IRS2+GKA; white squares) (n=8). **c** Blood glucose levels during the OGTT in the WT group (black circles), WT+GKA group (black squares), IRS2 group (white circles) and IRS2+GKA group (white squares) (n=7 or 8). **d** Area under the curve of the glucose excursion during the OGTT in the mice on the HF diet (white bars) or on the 0.04% GKA HF diet (black bars) (n=7 or 8). **e** Quantification of beta cell mass. Histological analysis of pancreatic islets from the mice on the HF diet (white bars) and the 0.04% GKA HF diet (black bars) (n=4 or 5). **f, g** Replication rates, assessed by BrdU incorporation after administration of GKA for 3 days, were determined in (**f**) WT mice and (**g**) *Irs2*$^{-/-}$mice after 10 weeks on the HF diet. Results are shown as vertical scatter plots for the wild-type mice without GKA (white circles) and with GKA (black triangles), and *Irs2*$^{-/-}$ mice without GKA (white diamonds) and with GKA (black circles) (n=4–11). Values are mean ± SE. *p<0.05; **p<0.01

the chronic reduction in ambient blood glucose levels induced by the GKA treatment rather than to the deficiency of IRS2. To investigate this possibility, we evaluated beta cell proliferation after administering the GKA on three consecutive days to mice fed the HF diet for 10 weeks; the results showed a significant decrease in the fed blood glucose level of both the wild-type and *Irs2*$^{-/-}$ mice shortly after administration of the GKA (data not shown). The BrdU incorporation ratio was significantly increased in the wild-type mice given the GKA for 3 days in comparison with the wild-type mice not given the GKA; this was not, however, seen in the *Irs2*$^{-/-}$ mice (Fig. 3f, g). These results support the concept that IRS2 could have an effect on beta cell proliferation stimulated by a GKA in vivo.

Effect of the GKA on the beta cell function of Irs2$^{-/-}$ *mice* To investigate the effect of the GKA on beta cell function ex vivo, we evaluated glucose-stimulated insulin secretion by the islets of *Irs2*$^{-/-}$ mice. Insulin secretion by *Irs2*$^{-/-}$ islets in response to 5.6 mmol/l glucose was significantly increased in the presence of GKA (Fig. 4a). The increase in insulin secretion in response to the application of 22 mmol/l glucose was less evident, suggesting that the secretion had peaked. These findings indicated that the GKA

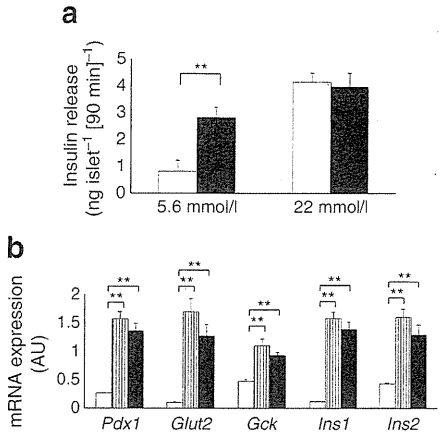

Fig. 4 Impact of GKA on glucose-stimulated insulin secretion ex vivo and changes in expression of genes involved in beta cell function in islets isolated from *Irs2*$^{-/-}$ mice. **a** Insulin secretion was measured with 5.6 mmol/l or 22 mmol/l glucose in the absence or presence of GKA. Results are shown as nanograms of insulin islet^{-1} 90 min^{-1} (n=7). Values are mean ± SE of data obtained from the analysis of islets isolated from *Irs2*$^{-/-}$ mice treated with vehicle (white bars) or 6 μmol/l GKA (black bars). **b** mRNA levels of *Pdx1*, *Glut2*, *Gck*, *Ins1* and *Ins2* in islets from *Irs2*$^{-/-}$ mice were measured by real-time quantitative PCR. Data have been normalised to beta-actin expression (white bars, 5.6 mmol/l glucose; hatched bars, 5.6 mmol/l glucose plus GKA; black bars, 22 mmol/l glucose) (n=3 or 4). Values are mean ± SE. **p<0.01

had stimulated glucose-stimulated insulin secretion by increasing glucose sensitivity without altering maximum insulin secretion by the *Irs2*$^{-/-}$ islets, which is consistent with our previous findings in wild-type and *Gck*$^{+/-}$ islet cells [11].

Next, we investigated whether the GKA affected the expression of genes involved in beta cell function in islets isolated from *Irs2*$^{-/-}$ mice. *Pdx1* mRNA significantly increased with 22 mmol/l glucose in comparison with 5.6 mmol/l glucose, and the GKA stimulated *Pdx1* mRNA expression at 5.6 mmol/l glucose in the isolated islets of *Irs2*$^{-/-}$ mice (Fig. 4b). In addition, there were no differences in *Pdx1* expression 5.6 mmol/l glucose in wild-type and *Irs2*$^{-/-}$ mice, and *Pdx1* expression was significantly increased with 22 mmol/l glucose or by the GKA in both genotypes of mouse to the same degree (data not shown). The increased *Pdx1* expression also paralleled the upregulation of *Glut2*, *Gck*, *Ins1* and *Ins2* levels (Fig. 4b). These results indicated that GKA enhanced beta cell function at the transcriptional level independently of IRS2.

Effect of oxidative stress on GKA-induced Irs2 and Pdx1 expression Exposure to exogenous H_2O_2 is known to reduce glucose-induced insulin secretion by impairing mitochondrial metabolism in beta cells [24]. This knowledge prompted us to evaluate the effect of oxidative stress on GKA-induced changes in the expression of genes related to beta cell function and proliferation. We investigated GKA-stimulated *Irs2* and *Pdx1* expression after H_2O_2 preconditioning. H_2O_2 significantly inhibited the upregulation of *Irs2* and *Pdx1* induced by GKA (Fig. 5a, b), and the inhibition was prevented by prior administration of alpha-tocopherol plus ascorbate (Fig. 5c, d). These results indicated that oxidative stress prevented GKA affecting the expression of genes related to beta cell function and proliferation.

Effect of GKA on Irs2 and Pdx1 expression in db/db mice Based on the above results, we next evaluated the effect of GKA on *Irs2* and *Pdx1* expression in *db/db* mice, a well-known model of type 2 diabetes accompanied by obesity and characterised by increased insulin resistance and severe damage to the pancreatic beta cells. The levels of gene expression for the reduced-form NADPH oxidase complex were coordinately elevated in islets isolated from *db/db* mice in comparison with islets isolated from wild-type mice (Fig. 6a–c), and thus the islets from the *db/db* mice could be exposed to oxidative stress. In contrast to the islets isolated from the wild-type mice, GKA failed to increase *Irs2* and *Pdx1* expression in islets isolated from the *db/db*

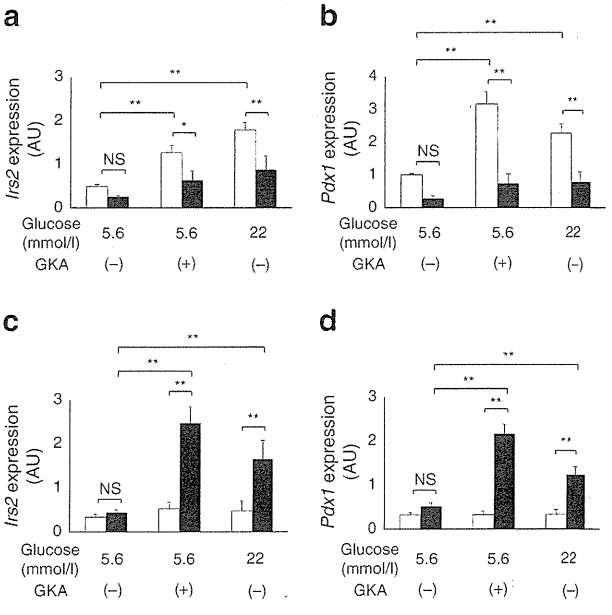

Fig. 5 Effect of GKA on changes in *Irs2* and *Pdx1* expression levels under oxidative stress. **a, b** mRNA levels of (**a**) *Irs2* and (**b**) *Pdx1* in islets from wild-type mice after H_2O_2 preconditioning were measured by real-time quantitative PCR. Isolated islets were incubated overnight with RPMI1640 medium containing 5.6 mmol/l glucose with or without 50 μmol/l H_2O_2 (white bars, absence of H_2O_2; black bars, presence of H_2O_2). **c, d** Effect of antioxidant treatment on GKA-stimulated *Irs2* (**c**) and *Pdx1* (**d**) expression. Isolated islets were incubated overnight with RPMI1640 medium containing 5.6 mmol/l glucose and 50 μmol/l H_2O_2 with or without alpha-tocopherol plus ascorbate (white bars, absence of alpha-tocopherol plus ascorbate; black bars, presence of alpha-tocopherol plus ascorbate). Data have been normalised to beta-actin expression (n=4). Values are mean ± SE. *p<0.05; **p<0.01

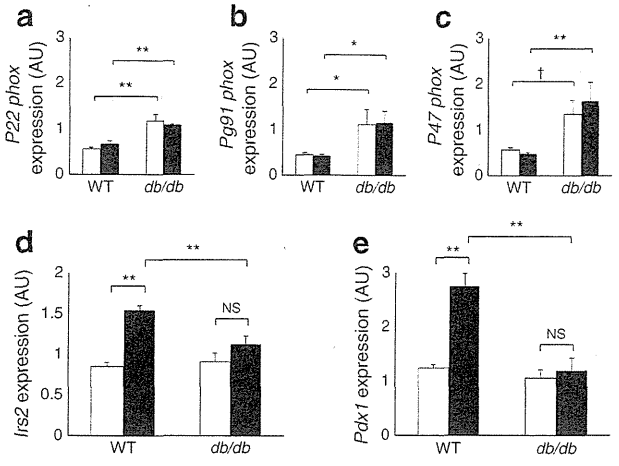

Fig. 6 Changes in expression of genes in isolated islets of *db/db* mice stimulated with GKA. mRNA levels of (**a**) *P22phox* (also known as *Cyba*), (**b**) *Pg91phox* (also known as *Cybb*), (**c**) *P47phox* (also known as *Ncf1*), (**d**) *Irs2* and (**e**) *Pdx1* in islets from 8-week-old wild-type and *db/db* mice were measured by real-time quantitative PCR. Data have been normalised to beta-actin expression (white bars, absence of GKA; black bars, presence of GKA) (n=4). Values are mean ± SE. *p<0.05; **p<0.01; †p=0.05

mice (Fig. 6d, e). These results showed that the effects of GKA on the expression of genes related to beta cell function and proliferation were diminished in the islets from the *db/db* mice.

Effect of exendin-4 on GKA-stimulated Irs2 and Pdx1 expression in db/db mice In order to increase *Irs2* and *Pdx1* expression stimulated by GKA in *db/db* mice, exendin-4 was intraperitoneally injected into *db/db* mice for 2 weeks before isolating the islets. Exendin-4 decreased blood glucose levels without affecting body weight (Fig. 7a, b). Remarkably, GKA was able to upregulate *Irs2* and *Pdx1* expression in the islets of *db/db* mice after prior administration of exendin-4 (Fig. 7c, d). It is noteworthy that exendin-4 alone was insufficient to upregulate these molecules. However, under our experimental conditions, the expression levels of genes for the reduced-form NADPH oxidase complex were unchanged (Fig. 7e–g).

Discussion

The results of the present study yielded three new findings. First, glucokinase activation by the GKA, a glucose-like activator of beta cell metabolism, increased IRS2 production; in addition, GKA-stimulated IRS2 production was able to affect beta cell proliferation, but not beta cell function. Second, the effects of the GKA on the expression of genes involved in beta cell function and proliferation were diminished in islets exposed to exogenous H_2O_2 and in those from *db/db* mice. Third, a combination of GKA and an incretin-related agent was effective in upregulating *Irs2* and *Pdx1* expression in these islets.

GKA increased the phosphorylation of CREB and IRS2 production (Fig. 1a, b), and 2-DG failed to increase *Irs2* expression by GKA (Fig. 1d). Both nifedipine and tacrolimus partly, but significantly, inhibited upregulation of *Irs2* expression by GKA (Fig. 1e, f). Taken together with the previous study [25], these results suggest that GKA increased CREB phosphorylation and *Irs2* expression in islets via glucose metabolism, Ca^{2+} influx and, in part, a Ca^{2+}–calcineurin pathway. In contrast, *Irs2* expression was not increased by either of the sulfonylureas. Sulfonylureas are known to close ATP-sensitive potassium channels regardless of glucose metabolism, and their closure results in membrane depolarisation, an influx of Ca^{2+} through voltage-dependent Ca^{2+} channels, and an increase in cytosolic free Ca^{2+} concentration, thereby triggering insulin secretion [26]. If that is true, why did the sulfonylureas fail to increase *Irs2* expression despite being able to increase the Ca^{2+} influx? One possible explanation is that the glucose flux per se may also be needed to increase *Irs2* expression and lead to beta cell proliferation [3, 22], since the sulfonylurea glibenclamide is unable to increase beta cell

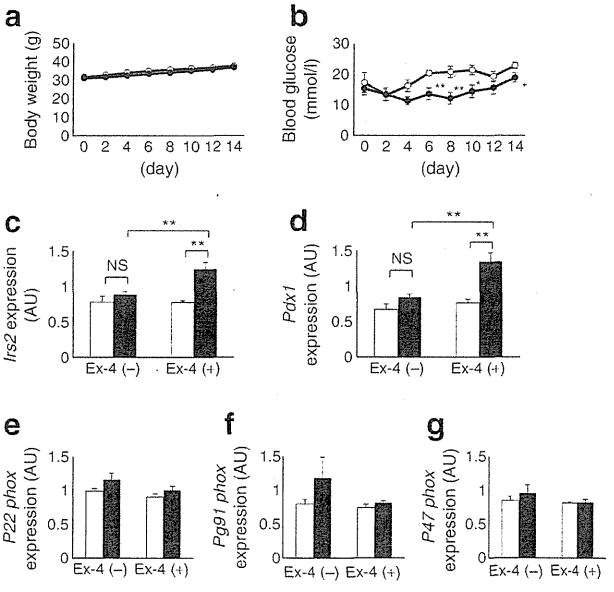

Fig. 7 Effect of a combination of exendin-4 and GKA on *Irs2* and *Pdx1* expression in *db/db* mice. **a, b** Changes in (**a**) body weight and (**b**) fed blood glucose levels of *db/db* mice injected or not injected with exendin-4 (Ex-4) for 2 weeks (white circles, not injected with Ex-4; black circles, injected with Ex-4) (n=8). The mRNA levels of (**c**) *Irs2*, (**d**) *Pdx1*, (**e**) *P22phox* (also known as *Cyba*), (**f**) *Pg91phox* (also known as *Cybb*) and (**g**) *P47phox* (also known as *Ncf1*) in islets from *db/db* mice were measured by real-time quantitative PCR. Data have been normalised to beta-actin expression (white bars, absence of GKA; black bars, presence of GKA) (n=5). Values are mean ± SE. *p<0.05; **p<0.01